LTE SYSTEM PERFORMANCE IN RELATION TO WIDEBAND CHANNEL PROPERTIES

DESI PRAMUDIWATI

Master of Science Thesis

Wireless and Mobile Communications Group
Department of Telecommunications
Faculty of Electrical Engineering, Mathematics and Computer Science
Delft University of Technology

TU Delft Delft University of Technology

TNO innovation for life

LTE SYSTEM PERFORMANCE IN RELATION TO WIDEBAND CHANNEL PROPERTIES

THESIS

Submitted in partial fulfilment of the requirements for the degree of

Master of Science

in

Electrical Engineering

by

Desi Pramudiwati

Committee Members**:**

Prof. Dr. Ir. Ignas Niemegeers (TU Delft)

Dr. Ir. Anthony Lo (TU Delft)

Dr. Ir. B.J. Kooij (TU Delft)

Dr. Haibin Zhang (TNO ICT)

Dr. Onno Mantel (TNO ICT)

Wireless and Mobile Communications Group

Department of Telecommunications

Faculty of Electrical Engineering, Mathematics and Computer Science

Delft University of Technology

Contents

List of Figures

List of Tables

List of Abbreviations

3GPP	3rd Generation Partnership Project
AMC	Adaptive Modulation and Coding
AoD	Angle of Departure
AoA	Angle of Arrival
AS	Angular Spread
AWGN	Additive White Gaussian Noise
BCH	Broadcast Channel
BLER	Block Error Rate
BS	Base Station
CCPCH	Common Control Physical Channel
CDD	Cyclic Delay Diversity
CP	Cyclic Prefix
CQI	Channel Quality Indicator
DL-SCH	Downlink Shared Channel
DS	Delay Spread
EESM	Exponential Effective SINR Mapping
EURO-COST	European Cooperative for Scientific and Technical Research
E-UTRAN	Evolved UMTS Terrestrial Radio Access Network
FDD	Frequency Division Duplex
FER	Frame Error Rate
FFT	Fast Fourier Transform
GSM	Global System for Mobile Communication
HARQ	Hybrid Automatic Repeat Request
HSPA	High Speed Packet Access
ISI	Inter Symbol Interference
ITU	International Telecommunication Union
LOS	Line of Sight
LTE	Long Term Evolution
MAC	Medium Access Control
MCH	Multicast Channel
MCS	Modulation and Coding Scheme
MIMO	Multiple Input Multiple Output
MISO	Multiple Input Single Output
MS	Mobile Station
NLOS	Non Line of Sight
OFDM	Orthogonal Frequency Division Multiplexing
PAPR	Peak to Average Power Ratio
PCH	Paging Channel

PDCCH	Physical Downlink Control Channel
PDSCH	Physical Downlink Shared Channel
PRB	Physical Resource Block
QAM	Quadrature Amplitude Modulation
QPSK	Quadrature Phase Shift Keying
RMS	Root Mean Square
SC-FDMA	Single Carrier Frequency Division Multiple Access
SCM	Spatial Channel Model
SFBC	Space-Frequency Block Codes
SIMO	Single Input Multiple Output
SISO	Single Input Single Output
SNR	Signal to Noise Ratio
TB	Transport Block
TDD	Time Division Duplex
TRI	Transmit Rank Indicator
TTI	Transmit Time Interval
UE	User Equipment
UMTS	Universal Mobile Telecommunication System
WLAN	Wireless Local Area Network

Acknowledgement

First of all, I would like to thank God, for blessing me that this graduation project can be done successfully. I would like to express my gratitude to Mr. Onno Mantel as the project manager for giving me the opportunity to take part on BEKAPLAN project and experience the real telecommunication engineering job at TNO ICT. I also express my gratitude to my daily supervisor, Mr. Haibin Zhang, for guiding me during this graduation project. Our discussion enriched my knowledge and broadened my way of thinking. I appreciate very much his understanding and patience. Then I would like to thank Mr. Remco Litjens and Mr. Yohan Toh for their kindness and help. Last but not least, I would like to thank Mr. Anthony Lo for his guidance in both technical knowledge and administrative procedures since I started until I finished this graduation project.

Abstract

In the current radio planning of wireless cellular networks, analysis of system performance is based on Signal to Noise Ratio (SNR). However, for wideband system such as LTE, the performance depends not only on the SNR but also on the amount of frequency and spatial diversity that the system can exploit. These diversities rely on the delay and angular profile of the radio channel which are often quantified in terms of delay spread (DS) and angular spread (AS). From an operator's point of view, in order to get reliable prediction of network capacity and coverage, delay spread and angular spread should therefore be taken into account in the radio planning. In this thesis, the effect of delay spread and angular spread on LTE system performance is investigated by performing LTE system level simulations. LTE system level simulation models AMC (Adaptive Modulation and Coding) hence it aligns with how the system works in reality. However, to implement AMC, system level simulation needs an accurate prediction of link level performance in terms of BLER. For this reason, AWGN link level simulation is required. The simulation results show that different delay spread values do not significantly affect the performance of LTE. This indicates that delay spread is not an important parameter to be taken into account in LTE radio planning. On the other hand, first result shows that per path angular spread strongly affects the performance of LTE. This suggests that it should be included in the radio planning of LTE.

Keywords: *delay spread, angular spread, AMC, LTE performance*

Chapter 1
Introduction

1.1 Background

LTE deployment worldwide

The continuous demand on high data rate and multimedia services motivated 3GPP to develop a new cellular wireless communication system called LTE (Long Term Evolution). LTE and its radio access technology called E-UTRAN (Evolved UMTS Terrestrial Radio Access Network) are expected to provide high speed data transmission, low latency, and high spectral efficiency as well as support for high mobility. These features support many demanding applications such as interactive TV, mobile video blogging, and advanced gaming. Moreover, LTE works on scalable bandwidth starting from 1.4MHz up to 20 MHz which makes it flexible for telecommunication operators to deploy this system.

The operator commitments to invest in LTE are growing faster than other technologies. In May 2011, 20 LTE networks in 14 countries were commercially available as shown in Table 1. In addition to this, 208 operators in 80 countries were investing in LTE network deployment and pre-commitment trials [1]. One of these countries is the Netherlands. The auction for LTE spectrum in the Netherlands was conducted in April 2010 with offered frequencies in the 2.6 GHz band. Of the 190 MHz bandwidth made available 135 MHz was reserved for newcomers. License for paired use or FDD (Frequency Division Duplex) was offered in blocks of 2x5 MHz whereas unpaired licenses used for TDD (Time Division Duplex) were offered in blocks of 5 MHz. The joint venture of Ziggo and UPC and Tele2 became the top bidders in this auction and won 2x20 MHz band. Meanwhile the incumbent operators, i.e. KPN, Vodafone, and T-Mobile were awarded 20 MHz, 20 MHz, and 10 MHz respectively. Only paired spectrum was sold and 69.7 MHz of unpaired spectrum was left unsold.

Table 1.1 Twenty commercial LTE networks in 14 countries till May 2011[1]

Country	Operator	Launched
Norway	TeliaSenora	15.12.09
Sweden	TeliaSenora	15.12.09
Uzbekistan	MTS	28.07.10
Uzbekistan	UCell	09.08.10
Poland	Mobyland & CenterNet	07.09.10
USA	MetroPCS	21.09.10
Austria	A1 Telekom Austria	05.11.10
Sweden	TeleNor Sweden	15.11.10
Sweden	Tele2 Sweden	15.11.10
Hong Kong	CSL Limited	25.11.10
Finland	TeliaSenora	30.11.10
Germany	Vodafone	01.12.10
USA	Verizon Wireless	05.12.10
Finland	Elisa	08.12.10
Denmark	Telia Senora	09.12.10
Estonia	EMT	17.12.10
Japan	NTT Docomo	24.12.10
Germany	Deutsche Telekom	05.04.11
Philippines	Smart Communication	16.04.11
Lithuania	Omnitel	28.04.11

Wideband channel properties affect MIMO and OFDM performance

In a wireless channel, transmitted signals experience reflection, diffraction, and scattering due to objects in the environment such as buildings, trees, people etc. Reflection, diffraction and scattering cause the signals to propagate through different paths. Some signals propagate through direct path which is often called Line of Sight (LOS) propagation, while some other signals propagate through non-direct path, which is called Non Line Of Sight (NLOS) propagation as depicted in Figure 1.1. The phenomenon that replicas of the transmitted signals arrived at the receiver through two or more different paths is called multipath propagation.

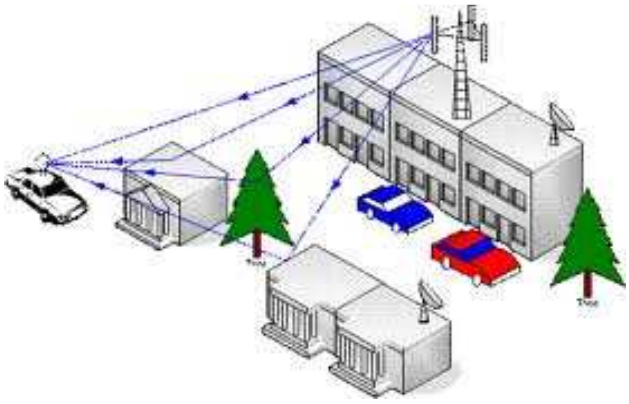

Figure 1.1 Multipath propagation in a wireless channel

Multipath propagation causes variations in time delay, amplitude, phase and angle of departure and arrival (AoD & AoA) of the received signals. Consequently, the received signal power fluctuates in space due to angular spread and/or in frequency due to delay spread and/or in time due to Doppler spread [2]. This fluctuation in signal level is called fading and generally degrades the performance of wireless communication systems.

Multipath propagation can be exploited as a benefit by MIMO (Multiple Input Multiple Output) in some circumstances and the impairment that it causes can be combated to a large extend by OFDM (Orthogonal Frequency Division Multiplexing). MIMO employs multiple antennas at different locations to take the advantage of different radio paths that exist. Hence, MIMO may result in higher capacity or quality compared to single antenna system. Because of this capability, MIMO has recently attracted much attention and is considered as a breakthrough in wireless communication [3]. On the other hand, OFDM separates the signal bandwidth into subcarriers yielding longer symbol duration. It reduces the effect of Inter Symbol Interference (ISI) introduced by multipath propagation.

In current radio planning of wireless cellular networks, analysis of system performance is based on signal to noise ratio (SNR) required to achieve a certain BLER (block error rate) target. This assumes narrowband systems where the effect of multipath is flat for the whole system bandwidth. However, for wideband OFDM systems, the effect of multipath is frequency selective. Thus the performance depends on the amount of frequency diversity that can be exploited. Meanwhile, for MIMO systems, the effect of multipath is exploited by different antennas by means of spatial diversity. Therefore, for MIMO-OFDM based systems such as LTE, the performance does not only depend on the SNR but also on the amount of frequency and spatial diversity that the system can exploit [4] [5]. These diversities rely on the delay and angular profiles of the channel which are often quantified in terms of delay spread (DS) and angular spread (AS) [6] [7]. From mobile operator's point of view, in order to get reliable prediction of network capacity and coverage, the impact of delay and angular spread to LTE performance should be taken into account in the LTE radio planning.

1.2 Objectives

The objectives of this study are:

1. To investigate the effect of wideband channel properties (more specifically delay spread and angular spread) on LTE system performance in terms of throughput
2. Based on the investigation results, provide recommendations for LTE radio planning

1.3 Contribution

The relations between wideband channel properties and the performance of LTE have been investigated in [8]. The investigation was done by performing link level simulations. However, LTE link level simulation does not model AMC (Adaptive Modulation and Coding). Hence, it does not align with how the system works in reality. **The main contribution of this study is the analysis of the effect of wideband channel properties (delay spread and angular spread) on LTE system performance by taking into consideration the implementation of AMC**.

In the Netherlands, LTE systems are still to be rolled out. In this phase, a radio planning is required in order to get an estimate of capacity and coverage of the network while at the same time maintains quality of services. The coverage and capacity estimation determines the cost of infrastructure provisioning. Hence, the estimation accuracy is important. Furthermore, this accuracy depends on the accuracy of propagation model used in the radio planning tool [9]. **And thus, the second contribution of this thesis is provide recommendations for radio planning based on more accurate propagation models taking into account wideband channel properties, i.e. delay spread and angular spread.**

1.4 Outline of the Master Thesis

This thesis is organized in 5 chapters including this introductory chapter.

Chapter 2 gives an introduction to LTE including its physical layer and key technologies. This chapter also provides an overview on radio propagation characteristics, wideband channel properties and Spatial Channel Model. In general, this chapter provides relevant background information from literatures.

Chapter 3 explains the approach taken in this study.

Chapter 4 describes the LTE system level simulation used in this study.

Chapter 5 provides the system level simulation results and the discussion on LTE system performance in relation to wideband channel properties.

Finally chapter 6 concludes this thesis and provides recommendations for future work.

Chapter 2
LTE and Radio Propagation

This chapter gives a summary of literature study that has been done. Section 2.1 provides overview of LTE (Long Term Evolution), followed by its physical layer structure and key technologies in section 2.2 and 2.3. Then radio propagation is given in section 2.4 which covers both large and small scale fading, wideband channel properties and spatial channel model.

2.1 Overview of Long Term Evolution

3GPP Long Term Evolution represents the latest standard in cellular network technology. It was designed to meet the continuous demands on high data rate, improved system capacity and coverage, low user latency and high user mobility [11]. The improved system performance ensures the competitiveness of LTE compared to other existing systems. Table 2.1 provides the main performance requirements to which the first release of LTE (3GPP Release 8) was designed compared to HSPA Release 6 performance [10]. These advanced performances can be achieved thanks to physical layer technologies such as MIMO (Multiple Input Multiple Output) and OFDM (Orthogonal Frequency Division Multiplexing) which will be explained in detail in section 2.3.

2.2 LTE Physical Layer

The LTE Physical Layer is highly efficient means of conveying both data and control information between an enhanced base station (called eNodeB in LTE terminology) and mobile user equipment (UE) [18]. Although the LTE physical layer specification describes both FDD (Frequency Division Duplex) and TDD (Time Division Duplex), the study in this thesis is focused on FDD, thus only LTE physical layer with FDD is discussed below. Furthermore, only downlink data transmission is considered.

Table 2.1 Summary of key performance requirement targets for LTE compared to HSPA [10]

DOWNLINK			
	LTE	**HSPA**	**Comment**
Peak transmission rate	>100 Mbps	7x14.4 Mbps	LTE in 20 MHz FDD, 2x2 spatial multiplexing. Reference: HSDPA in 5 MHz FDD, single antenna transmission
Peak spectral efficiency	> 5bps/Hz	3 bps/Hz	
Average cell spectral efficiency	>1.5-2.1 bps/Hz/cell	3-4 x 0.53 bps/Hz/cell	LTE: 2x2 spatial multiplexing, Interference Rejection Combining (IRC) receiver [3]. Reference: HSDPA, Rake receiver, 2 receive antennas
Cell edge spectral efficiency	>0.04-0.06 bps/Hz/user	2-3 x 0.02 bps/Hz	Assumed 10 users per cell
Broadcast spectral efficiency	> 1 bps/Hz	N/A	Dedicated carrier for broadcast mode
UPLINK			
Peak transmission rate	> 50 Mbps	5x11 Mbps	LTE in 20 MHz FDD, single antenna transmission. Reference: HSUPA in 5 MHz FDD, single antenna transmission
Peak spectral efficiency	> 2.5 bps/Hz	2 bps/Hz	
Average cell spectral efficiency	> 0.66-1.0 bps/Hz/cell	2-3x0.33 bps/Hz	LTE: single antenna transmission, IRC receiver. Reference: HSUPA, rake receiver, 2 receive antennas
Cell edge spectral efficiency	> 0.02-0.03 bps/Hz/user	2-3x0.01 bps/Hz	Assumed 10 users per cell
SYSTEM			
User plane latency (two way radio delay)	< 10 ms	<100 ms	
Connection set-up latency	< 50ms	May exceed 1000 ms	Dormant state→ active state
Operating bandwidth	1.4 – 20 MHz	5 MHz	(initial requirement started at 1.25 MHz)
VoIP capacity	NGNM preferred target is > 60 sessions/MHz/cell		

2.2.1 LTE Frame Structure

Figure 2.1 depicts the generic frame structure for uplink and downlink operation in LTE according to [12]. The duration of one frame in LTE system is 10 ms with each frame is divided into 10 sub-frames of 1 ms. Each sub-frame is further divided into two time slots, each with duration of 0.5 ms. Each time slot consists of either 7 or 6 OFDM symbols depending on the type of cyclic prefix (CP) employed.

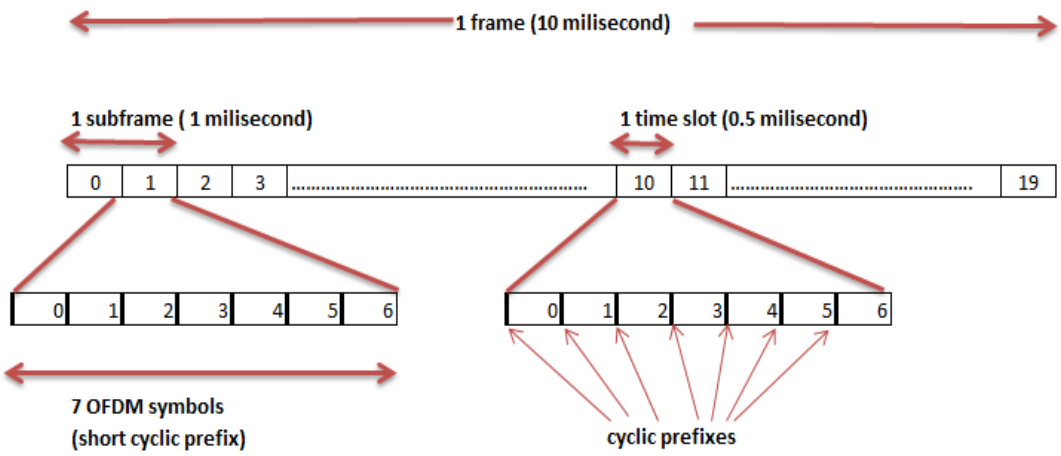

Figure 2.1 LTE Frame Structure with 7 OFDM symbols per time slot

Cyclic prefix (CP) is a copy of the last portion of the data symbol which is inserted in front of the same data symbol during the guard interval. LTE employed two types of cyclic prefix, namely normal CP and extended CP. The duration of normal CP and extended CP is given in Table 2.2. T_s is the standard sampling time unit used throughout the LTE specification documents and l is the index of OFDM symbol in a slot.

Table 2.2 Cyclic Prefix Duration

Configuration		Cyclic Prefix Length	
		Ts	μsec
Normal CP	$\Delta f = 15kHz$	160 for l = 0	5.21 for l = 0
		144 for l = 1,2,…5	4.69 for l = 1,2,5
Extended CP		512	16.67
		1024	33.33

In the case of FDD (Frequency Division Duplex), all sub frames are assigned either for downlink or uplink transmission as shown in Figure 2.2. The blue arrow represents downlink transmission and the black arrow represents uplink transmission.

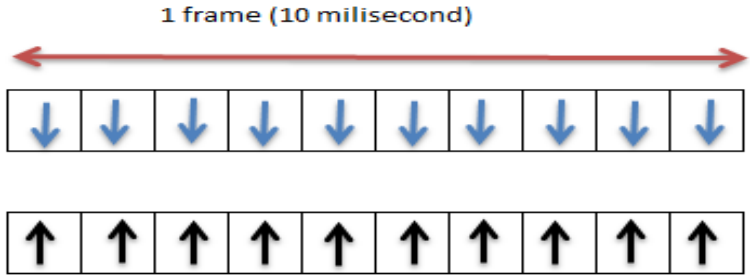

Figure 2.2 Uplink-Downlink Configurations for LTE FDD

As mentioned above, LTE uses OFDM as one of the key technologies. In OFDM, the whole transmission bandwidth is divided into subcarriers. Further, in LTE physical layer 12 consecutive

subcarriers are grouped into one PRB (Physical Resource Block). A PRB has duration of 1 time slot. Within one PRB there are 12x7 or 12x6 resource elements as depicted in Figure 2.3. A PRB is the smallest element allocated to a user. Table 2.3 provides total number of available PRBs for different spectrum bandwidth.

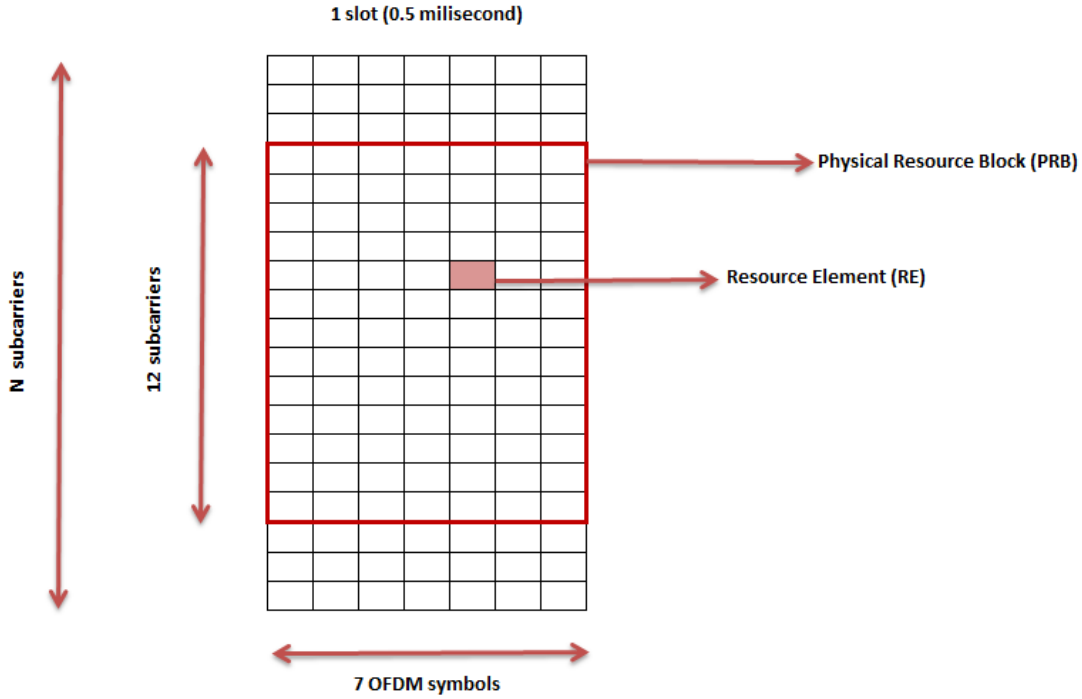

Figure 2.3 LTE downlink resource grid [12]

Table 2.3 Available PRBs for different bandwidth

Bandwidth (MHz)	**1.4**	**3**	**5.0**	**10.0**	**15.0**	**20.0**
Subcarrier bandwidth (kHz)	**15**					
Physical Resource Block (PRB) bandwidth (kHz)	**180**					
Number of available PRBs	**6**	**15**	**25**	**50**	**75**	**100**

2.2.2 LTE Downlink Reference Signal Structure

For terminal mobility and channel estimation purpose, reference signals are inserted into the PRBs. These signals are inserted in the first and the fifth OFDM symbol of each slot when the normal CP is used and in the first and fourth OFDM symbol when extended CP is used. Reference signals are sent on every sixth subcarriers. Figure 2.4 depicts the position of reference signals in a PRB.

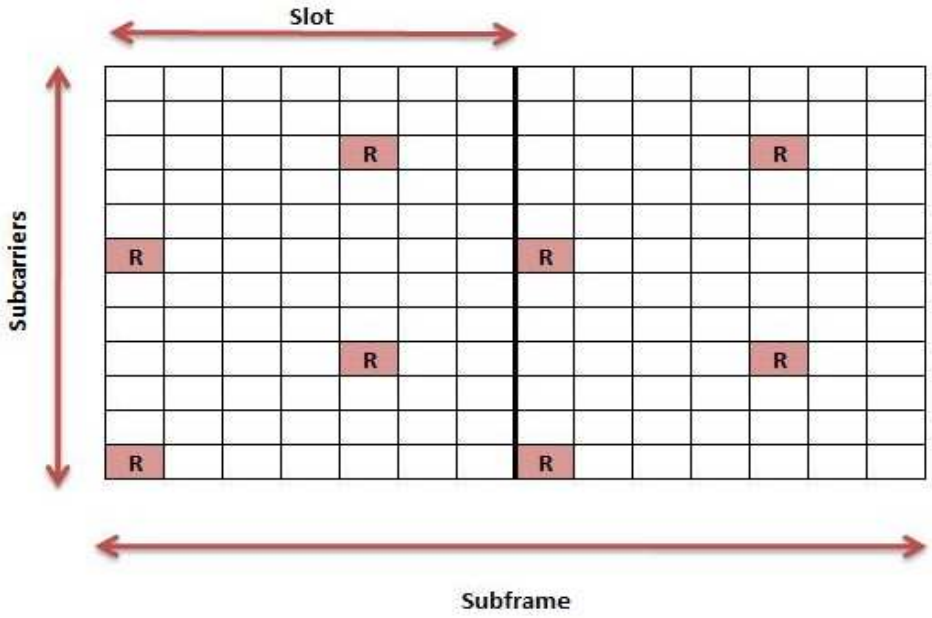

Figure 2.4 Position of reference signals in a PRB [12]

2.2.3 LTE Downlink Physical Channel

Physical channels convey information from higher layers in the LTE stack. Each physical channel defines algorithms for bit scrambling, modulation, layer mapping, CDD (Cyclic Delay Diversity) precoding and resource element assignment. There are three downlink physical channels in LTE.

Physical Downlink Shared Channel. PDSCH is designed for high data rate transmission such as data and multimedia services. It uses QPSK, 16 QAM and 64 QAM as the modulation schemes. Spatial multiplexing is exclusively implemented in this channel.

Physical Downlink Control Channel. PDCCH is used for UE-specific control information. Instead of high data rate requirement, robustness is more important for this channel. PDCCH is mapped into resource elements in up to the first three OFDM symbols in the first slot of each subframe. QPSK is the only modulation used in this channel.

Common Control Physical Channel. CCPCH carries cell-wide information. Same as PDCCH, robustness is more important for this channel and QPSK is the only modulation scheme used. CCPCH is transmitted close to the center frequency.

2.2.4 LTE Downlink Transport Channel

In LTE Physical Layer, transport channels act as service access point (SAPs) for higher layers. There are four downlink transport channels in LTE system.

Broadcast Channel. BCH is used to broadcast the system parameters such as random access related parameters to enable the device accessing the system. It has fixed format and must be broadcast over entire coverage area of a cell.

Downlink Shared Channel. DL-SCH carries user data information for point to point connection in the downlink. It supports Hybrid ARQ (HARQ) and dynamic link adaptation by varying modulation, coding and transmit power. It is suitable for transmission over entire cell coverage area and use with beamforming. It supports dynamic and semi-static resource allocation and also discontinuous receive (DRX) for power save.
Paging Channel. PCH is used to carry paging information. It supports discontinues receive (DRX) in user equipment (UE). It is a requirement for broadcast over entire cell coverage area and is mapped to dynamically allocated physical resources.
Multicast Channel. MCH is used to transfer multicast data to the UE in the downlink. Same as PCH, MCH is a requirement for broadcast over entire cell coverage area. It supports MB-SFN and semi-static resource allocation.

2.2.5 Mapping Downlink Physical Channel to Downlink Transport Channel

Transport channels are mapped to physical channels as shown in Figure 2.5. PCH and DL-SCH are mapped to PDSCH. BCH is mapped to CCPCH. It is now under consideration that BCH and MCH is mapped to PDSCH.

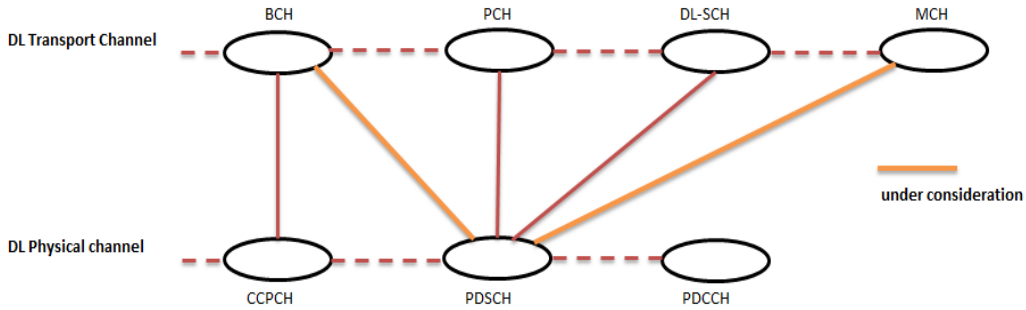

Figure 2.5 Mapping Downlink Transport Channels to Physical Channels

2.3 LTE key technologies

2.3.1 Multiple Input Multiple Output (MIMO)

As the name implies, MIMO system employs multiple antennas at both transmitter and receiver. Figure 2.6 depicts a diagram of a MIMO wireless transmission system with N transmit antennas and M receive antennas. The idea behind MIMO is that the signals on the transmit antennas at one end and the received antennas at the other ends are combined in such a way that the quality of the communication for each MIMO user will be improved [3]. The improved quality can be quantified in terms of error rate or throughput (data rate) depending on how MIMO combines the signals.

A key feature for MIMO is its ability to turn multipath propagation, traditionally a problem in wireless communication, into a benefit for the user. MIMO effectively takes the advantages of random fading [13] [14]. In the presence of random fading, the probability of losing the signal decrease with the number of decorrelated antenna elements being used [3]. Thus, in MIMO, one of key parameters which determines the performance is the spatial correlation between antenna elements. This spatial correlation determines the independency between antenna elements and thus the amount of spatial diversity that can be exploited.

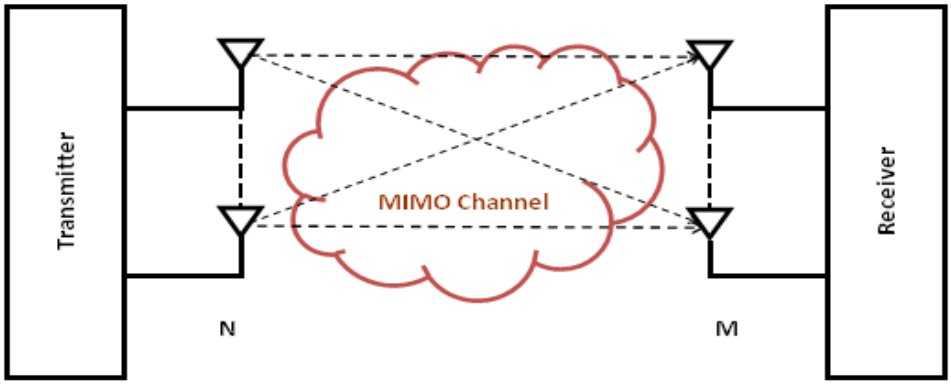

Figure 2.6 Block diagram of MIMO wireless transmission system

Capacity of MIMO

According to Shannon theory, the capacity of a system using single antenna at both the transmitter and the receiver or often called SISO (Single Input Single Output) system is given by [3]:

$$C_{SISO} = \log_2(1 + \rho|h|^2)\ bit/s/Hz \qquad (2.1)$$

where h is complex gain of the fixed wireless channel or that of praticular realization of random channel and ρ is the SNR at any Rx antenna. When more antennas are deployed at the receiver, the system becomes single input multiple output (SIMO) and the capacity is given by [3]:

$$C_{SIMO} = \log_2\left(1 + \rho \sum_{i=1}^{M}|h_i|^2\right) \quad bit/s/Hz \qquad (2.2)$$

Where h_i is the channel gain between the transmitter and the receive antenna i. From the above equation it can be seen that by implementing SIMO the capacity of the system increases logarithmically with the number of receive antennas. Similarly, when more antennas are implemented in the transmitter, the system becomes MISO (Multiple Input Single Output) and the capacity is given by [3]:

$$C_{MISO} = \log_2\left(1 + \frac{\rho}{N}\sum_{i=1}^{N}|h_i|^2\right) \quad bit/s/Hz \tag{2.3}$$

Where h_i is the channel gain between the transmitter *i* and the receive antenna. The normalization by N ensures that the total transmitted power is fixed. Again, the capacity of the system has a logarithmic relationship with the number of transmit antennas. Furthermore, when N antennas are employed at the transmitter and M antennas are employed at the receiver giving rise to MIMO systems, the diversity is exploited in both transmitter and receiver yielding a famous capacity equation [3] [13] [14] [15]

$$C_{MIMO} = \log_2\left[det\left(I_M + \frac{\rho}{N}HH^*\right)\right] \quad bit/s/Hz \tag{2.4}$$

Where * means transpose-conjugate, *H* is MxN channel matrix and I_M is identity matrix with size of M. The equation 2.4 assumes equal power among transmitter antennas. It is investigated in [13] and [14] that the capacity grows linearly with *m = min (M, N)* rather than logarithmically as in the case of SIMO and MISO.

MIMO modes standardized in LTE

MIMO performance depends on a number of factors such as the characteristic of wireless channel, e.g. low or high scattering, the signal quality (as measured by SINR), and the correlation of the received signals at the receive antennas. Certain MIMO modes will be more effective than others depending on these factors.

Before explaining each of the mode standardized in LTE, some terminologies are introduced below:

- **Spatial Layer** is the term used in LTE for the different streams generated by spatial multiplexing. It can be described as a mapping of symbols onto the transmit antenna ports.
- **Rank** of the transmission is the number of layers transmitted.
- **Codeword** is an independently encoded data block, corresponding to a single Transport Block (TB) delivered from Medium Access Control (MAC) layer to Physical layer.

Transmission modes in the first release of LTE according to [16] [17] are:

- Mode-1, single antenna port
  In this mode, single data stream is transmitted from single antenna and received by another single antenna (SISO).
- Mode-2, transmit diversity
  Instead of transmitting from one single antenna, the same data stream is transmitted from multiple antennas and is coded differently in each antenna using so called 'Space-Frequency Block Codes'. Instead of repeating the data symbols in time, SFBC repeat the

data symbols over different subcarrier on each antenna. This mode is used by default for the common channel as well as for control and broadcast channel. Since it is single layer tranmission, the peak rate is not improved. But the quality becomes more robust and lower SNR is required to decode the signal.

- Mode-3, open loop spatial multiplexing
  This mode involves the transmission of two information streams (two code words) over two or more antennas (up to four in LTE). There is no feedback from the user equipment (UE) but the Transmit Rank Indication (TRI) transmitted by UE is used by base station to select the number of spatial layers. Since multiple data streams are transmitted, open loop spatial multiplexing results in better throughput than transmit diversity.
- Mode-4, closed loop spatial multiplexing
  Similar to open loop spatial multiplexing, in this mode, two information streams are transmitted over two or more transmit antennas. The difference is in the feedback from UE to the BS. This feedback allows BS to pre-code the data in order to optimize the transmission over the wireless channel so the received data stream can be easily separated into the original data stream by the receiver.
- Mode-5, multi user MIMO
  This mode is similar to closed loop spatial multiplexing, but the data streams are targeted to different users. While the data rate per user may be same, the overall network data rate is increased. The number of spatial layer limits the number of users. The users are separated in space domain and can be uncorrelated due to individual beam-forming patterns. If the layers are not completely orthogonal, then each user may experience interference from other users.
- Mode-6, closed loop rank 1 with pre-coding
  This mode involves the transmission of a single data stream over a single spatial layer. In this mode, the UE feeds channel information back to the BS to indicate appropriate precoding to apply for the beamforming operation.
- Mode-7, single antenna port
  This is a beamforming mode where a single data stream is transmitted over a single spatial layer. A dedicated reference signal forms another antenna port, i.e. port 5 and allows transmission from more than 4 antennas.

Among the above mentioned transmission modes, only three modes are investigated in this study: single antenna (SISO), open loop spatial multiplexing, and transmit diversity. But the transmit diversity mode is combined with receive diversity yielding an additional mode of “transmit receive diversity”. Another mode implemented in the study is receive diversity which assumes two antennas at the UE and maximal ratio combining is employed to combine the received signals.

2.3.2 Orthogonal Frequency Division Multiplexing (OFDM)

A critical factor for the good performance of wireless communication is the choice of an appropriate modulation and multiple access technique [10]. Recent broadband communication

systems such as Wimax and LTE use OFDM as the modulation technique. OFDM is a specific type of multicarrier modulations which provides high spectral efficiency. This efficiency is achieved by dividing the whole system bandwidth into subcarriers which are orthogonal among each other. Figure 2.7 shows the spectrum of an OFDM signal.

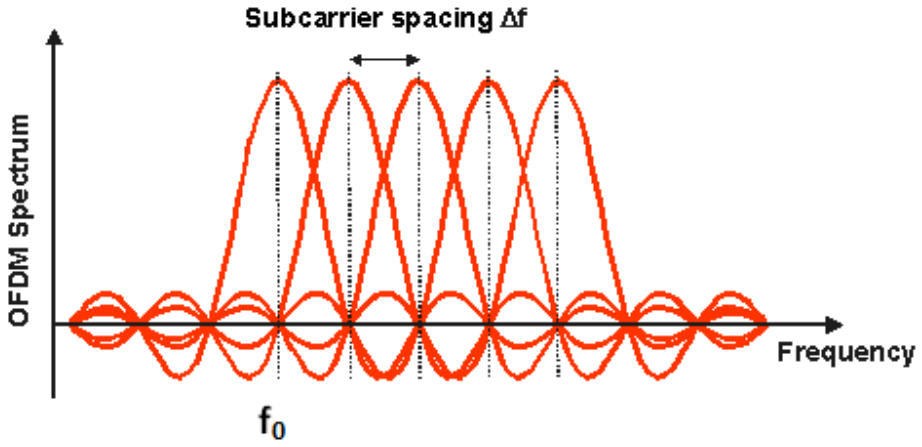

Figure 2.7 Spectrum of an OFDM system

In OFDM, a high rate data stream is first converted into M parallel information stream with data rate of R/M as shown in Figure 2.8. Thus the symbol duration increases by a factor of M such that it becomes longer than the typical channel delay spread. Then each information stream modulates a subcarrier. The frequency of m^{th} carrier is

$$f_m = f_0 + \frac{m}{T} \qquad m = 0, 1, 2, \ldots\ldots\ldots\ldots, M-1 \tag{2.5}$$

Where f_0 is the lowest frequency of the subcarrier and T is the symbol duration. Thus the multicarrier transmitted signal is written as [15]

$$s(t) = \sum_{m=0}^{M-1} \sum_{i=-\infty}^{\infty} b_m(i)\, e^{j2\pi f_m(t-iT)}\, p(t-iT) \tag{2.6}$$

Where $b_m(i)$ is the symbol of the m_{th} subchannel at time interval iT and $p(t)$ is the response of the transmitter filter which is a rectangular pulse with duration T and amplitude 1.

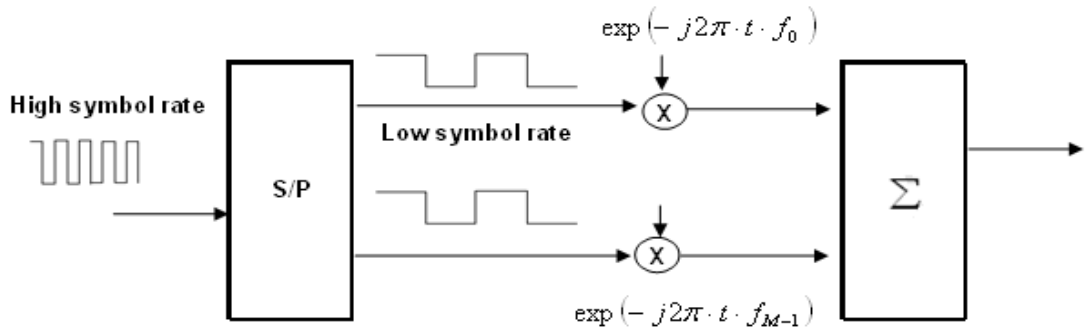

Figure 2.8 Serial to parallel conversion operation for OFDM

A major feature of OFDM that made it chosen as a key technology for LTE is it's ability to combat the severe effect of multipath propagation. The delay induced by multipath propagation can cause a symbol received along a delayed path to interfere the subsequent symbol arriving at the receiver via a more direct path [18]. This effect is reffered to as inter-symbol interference (ISI) as depicted in Figure 2.9.

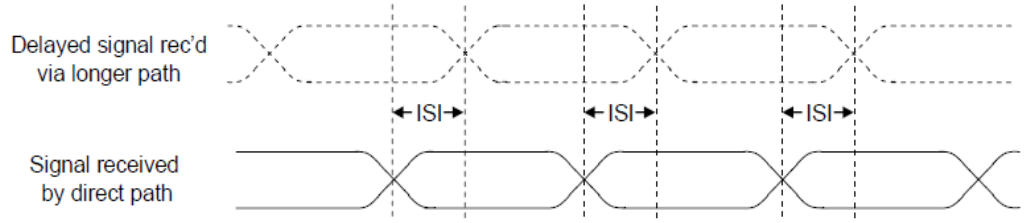

Figure 2.9 Multipath induced time delay result in ISI

In a high-rate data stream, the symbol duration is shorter than the typical delay spread. Thus it is prone to ISI which can be solved by means of complex channel equalization. On the other hand, OFDM devides the whole system bandwidth into subcarriers which have small bandwidth. Hence the symbol duration in each subcarrier becomes longer and it can mitigate the bad effect of ISI. Moreover, OFDM inserts cyclic prefix (CP) in the data symbol during the guard interval as shown in Figure 2.10. There are two components of OFDM symbol, cyclic prefic and FFT period. Within the CP, it is possible to have distortion from the previous symbol. But, when the length of CP exceeds the maximum access delay of the multipath propagation channel, the previous symbol doesn't spill into the FFT period. Therefore ISI can be eliminated.

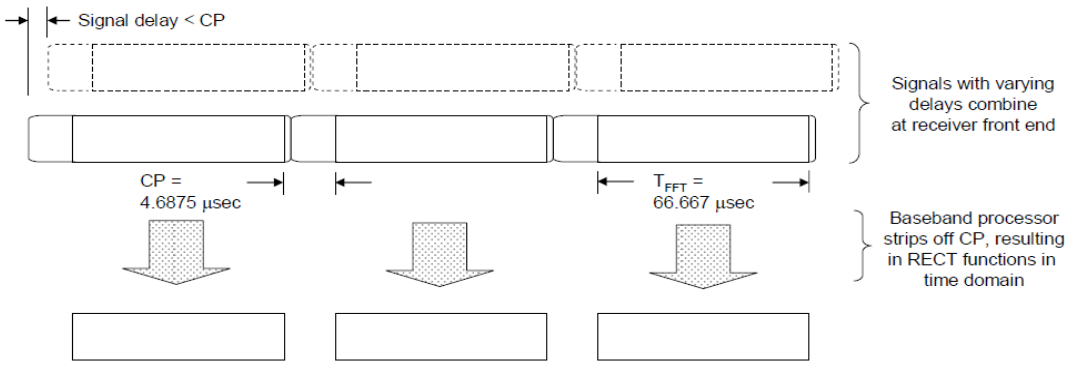

Figure 2.10 OFDM Eliminates ISI via Longer Symbol Periods and a Cyclic Prefix

Inspite of its remarkable features, OFDM has some drawbacks. A major drawback is that it has high signal peak to average power ratio (PAPR). The instantaneous transmitted power can vary dramatically within one OFDM symbol. This reduces the efficiency of the transmitter RF power amplifier. Because of this drawback, OFDM is only implemented in LTE downlink data transmission as the power consumption is a key consideration for UE terminals. Meanwhile for uplink transmission, SC-FDMA (Single Carrier-Frequency Domain Multiple Access) is chosen as the multiple access technique since it offers the same degree of multipath protection as OFDM, but the PAPR is lower.

2.4 Radio Propagation

During the propagation in a wireless channel, transmitted signals experience reflection, diffraction and scattering. Reflection occurs when radio waves hit a smooth surface which has a very large dimension compared to the the signal wavelength (λ). Diffraction occurs when the radio path between the transmitter and the receiver is obstructed by a solid object with a dimension large compared to λ, yielding another waves to be formed behind the obsturcting object. Scattering occurs when radio waves hit either a large and rough surface or any surface whose size is in the order of λ or less, causing the signal to be spread out (scatter) in all direction. Due to these three phenomenons, there is a fluctuation in the received signal strength which is often called fading. In the next subsection, large scale and small scale fading will be discussed.

2.4.1 Large Scale and small scale fading

Large scale fading represent the average signal power attenuation due to motion over large areas [19]. This phenomenon is caused by terrain contours between transmitter and receiver such as mountain, hills, building, etc. Large scale fading is often represented statistically in terms of path loss which is a function of distance and a log normally distributed variation about the mean pathloss which is often called shadowing (shadow fading). A number of empirical models were

developed to model the relationship between the distance and path loss for different environment. This empirical model will be provided in more detail in the section 2.4.2.

Small scale fading refers to the dramatic changes in signal amplitude and phase that can be experienced as a result of small changes (as small as a half wavelength) in the spatial separation between a receiver and a transmitter. Sometimes it is called multipath fading because the fading is caused by multipath propagation. Small scale fading envelope can be described by Rayleigh distribution if the multiple reflective paths are large in number and there is no line of sight signal component. But when there is a dominant non fading signal component present, such as line of sight propagation, the small scale fading envelope is described by Rician distribution. Figure 2.11 depicts the comparation between small scale fading and large scale fading.

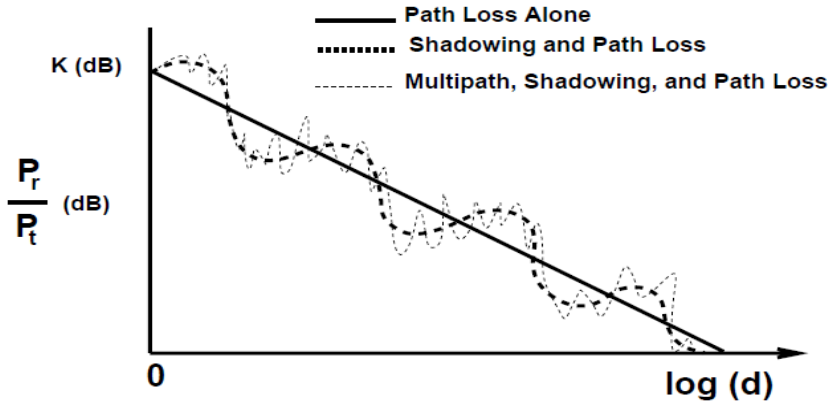

Figure 2.11 Path Loss, Shadowing and Multipath Fading versus distance [29]

2.4.2 Empirical Path Loss Model

The Okumura Model

One of the most common model for urban macrocell is Okumura model [29]. This model works for frequency range of 150-1500MHz, distance of 1-100 Km and assumed BS height of 30-100 m. Okumura used measurement of signal attenuation from base station to mobile station in Tokyo to create set of curves of signal attenuation relative to free space propagation in irregular terrain. The empirical pathloss of Okumura is given as:

$$P_L(d)\ dB = L(f_c, d) + A_{mu}(f_c, d) - G(h_r) - G_{AREA} \qquad (2.7)$$

Where $L(f_c, d)$ is free space path loss at distance d and carrier frequency f_c , $A_{mu}(f_c, d)$ is the median attenuation in addition to free path loss across all environments, $G(h_t)$ is the base station antenna height gain factor, $G(h_r)$ is the mobile antenna height gain factor, and G_{AREA} is a gain

factor generated by the environment in which the system is operating and obtained from Okumura's empirical plots. $G(h_t)$ and $G(h_r)$ are defined as:

$$G(h_t) = 20\log_{10} h_t/200, \qquad for\ 30m < h_t < 1000m$$

$$G(h_r) = \begin{cases} 10\log_{10} h_r/3, & for\ h_r < 3m \\ 20\log_{10} h_r/3, & for\ 3m < h_r < 10m \end{cases}$$

Hata Model

Hata model is an empirical formulation of the graphical path loss provided by Okumura [29]. The parameters in this model are same as under the Okumura model. The empirical pathloss in urban areas under Hata model is given as:

$$P_{L,urban}\ dB = 69.55 + 26.16\log_{10}(f_c) - 13.82\log_{10}(h_t) - a(h_r) + (44.9 - 6.55\log_{10}(h_t)) \qquad (2.8)$$

Where $a(h_r)$ is a correction factor for mobile antenna height based on the size of the coverage area and given by:

$$a(h_r) = \begin{cases} (1.1\log_{10}(f_c) - 0.7)h_r - (1.56\log_{10}(f_c) - 0.8)\ dB, for\ small\ to\ medium\ cities \\ 3.2(\log_{10}(11.75h_r))^2 - 4.97\ dB, \qquad for\ f_c \geq 300\ MHz\ in\ large\ cities \\ 8.29(\log_{10}(1.54))^2 - 1.1\ dB, \qquad for\ f_c \leq 300\ MHz\ in\ large\ cities \end{cases}$$

For suburban and rural area, corrections to urban area are made, thus the empirical pathloss models become:

$$P_{L,suburban}\ (d) = P_{L,urban}(d) - 2\left[\log_{10}\left(\frac{f_c}{28}\right)\right]^2 - 5.4 \qquad (2.9)$$

and

$$P_{L,rural}(d) = P_{L,urban}\ (d) - 4.78[\log_{10}(f_c)]^2 + 18.33\log_{10}(f_c) - K \qquad (2.10)$$

Where K ranges from 35.94 (countryside) to 40.94 (desert). The Hata model provides good approximation with Okumura model for distance d > 1km. Hence it is a good estimate for first generation cellular system but not for current cellular system with smaller cell sizes and higher frequency.

COST 231 Extension to Hata Model

European cooperative for scientific and technical research (EURO-COST) extended the Hata model as follows [29]:

$$P_{L,urban}\,(d)\;dB = 46.3 + 33.9\,\log_{10}(f_c) - 13.82\log_{10}(h_t) - a(h_r) + (44.9 - 6.55\log_{10}(h_t))\log_{10}(d) + C_M \quad (2.11)$$

Where C_M is 0 dB for medium sized cities and suburbans and 3 dB for metropolitan area. Parameters for this model are as follows: 1.5 GHz < f_c< 2 GHz, 30m <h_t < 200m, 1m < h_r < 10m and 1Km < d <20 Km.

2.4.3 ITU and 3GPP Multipath Channel Model

ITU multipath models are empirical channel model that are specified in [20]. There are three different environments specified in the recommendation, namely indoor office, outdoor-to-indoor pedestrian and vehicular. In this research, pedestrian and vehicular multipath model are used along with 3GPP multipath model, typical urban. These multipath models are described in detail as follows.

Pedestrian A, B

Pedestrian environment is characterized by small cells and low transmit power. Base stations with low antenna height are located outdoors while pedestrian users are located on the streets and inside buildings and residences. The mobile speed is assumed to be 3 km/hr. In the case of line of sight, the path loss exponent is 2 but a range up to 6 maybe encountered due to trees and other obstructions. The number of paths in Pedestrian A model is 4 while in Pedestrian B model is 6. The average powers and relative delays for the taps of multipath channels based on ITU recommendations are given in Table 2.4.

Table 2.4 Average Powers and Relative Delays of ITU Multipath Pedestrian A and Pedestrian B Models

Tap no.	Pedestrian A		Pedestrian B	
	Relative delay (ns)	Average Power (dB)	Relative Delay (ns)	Average Power (dB)
1	0	0	0	0
2	110	-9.7	200	-0.9
3	190	-19.2	800	-4.9
4	410	-22.8	1200	-8
5	NA	NA	2300	-7.8
6	NA	NA	3700	-23.9

Vehicular A

Vehicular environment is characterized by large cells and higher transmit power. Received signal is composed of multipath components with NLOS case only. Received signal power decreased with distance and path loss exponent is 4 for both urban and suburban area. In rural areas, path loss may be lower than in urban and suburban area while in mountainous area, path loss exponent

is close to 2. The mobile speed is assumed to be vehicular speed at about 120 km/h. The average powers and relative delays for the taps of multipath channel based on ITU recommendations are given in Table 2.5.

Table 2.5 Average Power and Relative Delays for ITU Multipath Vehicular A Model

Tap no.	Vehicular A	
	Relative delay (ns)	Average Power (dB)
1	0	0
2	310	-1.0
3	710	-9.0
4	1090	-10.0
5	1730	-15.0
6	2510	-20.0

3GPP Typical Urban Multipath Model

Typical Urban is one of the multipath models commonly used for GSM system in the cellular and PCS bands. There are two definitions of Typical Urban model which has 12 delay taps and 6 delay taps respectively. Both definitions have the same delay spread value. In this research, typical urban model with 6 delay taps is used. Table 2.6 and 2.7 show the average powers and relative delays for Typical Urban with 12 taps and 6 taps respectively.

Table 2.6 Power and Relative Delays for Typical Urban Model with 12 delay taps

Tap no.	Typical Urban	
	Relative delay (ns)	Average Power (dB)
1	0	-4
2	0.1	-3
3	0.3	0
4	0.5	-2.6
5	0.8	-3
6	1.1	-5
7	1.3	-7
8	1.7	-5
9	2.3	-6.5
10	3.1	-8.6
11	3.2	-11
12	5	-10

Table 2.7 Average Power and Relative Delays for Typical Urban Model with 6 delay taps

Tap no.	Typical Urban	
	Relative delay (ns)	Average Power (dB)
1	0	0.189
2	0.2	0.379
3	0.5	0.239
4	1.6	0.095
5	2.3	0.061
6	5.0	0.037

2.4.4 Delay Spread

Due to the reflection, diffraction and scattering by objects in the environment, transmitted signal propagates through different paths. Thus replicas of the transmitted signal arrive at the receiver with different time delays. This time delay variation is often quantified in terms of delay spread. Larger delay spread means there is a large variation in time delays of different multipath components. According to a measurement conducted by TU Eindhoven in the vicinity of Amsterdam Arena, the observed delay spread varies from 0 up to 500 ns [21]. Another measurement conducted by AWE Communication and NOKIA observed that delay spread varies in the range of 0 up to 1500 ns [22]. This difference may be due to the difference in the distance between the transmitter and the receiver in these two measurements.

Delay spread is mathematically quantified in the root mean square value as provided by the equation 2.12 below:

$$T_\sigma = \sqrt{\frac{\sum_n (t_n - \bar{T})^2 . P_n}{\sum_n P_n}} \tag{2.12}$$

Where

$$\bar{T} = \frac{\sum_n t_n . P_n}{\sum_n P_n}$$

T_σ is the rms of delay spread, t_n is the delay of the n^{th} path and P_n is the power of the n^{th} path.

Delay spread affects OFDM Performance

The relation between delay spread and OFDM performance can be explained by the principle of frequency diversity. Delay spread is inversely proportional to coherence bandwidth, i.e. larger delay spread results in smaller coherence bandwidth. Coherence bandwidth is the bandwidth over which the channel is considered to be “flat”. Within the coherence bandwidth, different signals experience the same channel frequency response. The fading characteristics within coherence bandwidth is flat, thus it is called flat fading. If the bandwidth of a signal is larger than the channel coherence bandwidth, the channel is considered as frequency selective channel. Signals

with frequency difference more than coherence bandwidth experience different fading. Therefore, it is called frequency selective fading.

Current OFDM systems often work on frequency selective channel. When OFDM signals are transmitted over a frequency selective channel, the data transmitted on different subcarriers experience a different channel response. Some subcarriers may experience deep fading, while others not. By using frequency domain forward error correction (channel coding) and interleaving across all subcarriers, the defected data are still recoverable since the data in the non-defected subcarriers are mostly error free. And thus frequency diversity is exploited. It is expected that generally the performance of OFDM is better for larger delay spread.

There are some literatures which have investigated the effect of delay spread on the performance of OFDM-based system. Various performance metrics are used in the investigations, such as block error rate, throughput and the amount of transmit power. In [8] the effect of delay spread on LTE performance has been examined by using exponential Power Delay Profile (PDP) channel model in SISO transmission. The result in Figure 2.12 shows that larger delay spread introduces lower block error rate. In other words, to achieve the same block error rate, less SNR is required when delay spread is larger. This is due to the advantage of more frequency diversity introduced by larger delay spread as explained in some previous paragraphs. In [23] the performance of different scheduling algorithms and power allocation methods are investigated in a system which consists of one base station and multiple users for the European WLAN alternative HiperLAN/2 (similar to IEEE 802.11a). One of the results shows the effect of delay spread on throughput of OFDM system as depicted in Figure 2.13. It is shown that throughput depends on delay spread especially in the region of low delay spread. An investigation on delay spread effect on the transmit power of OFDM system with 16 QAM modulation has been done in [24]. The results shows that transmit power (required for a certain QoS) decreases with the increase of delay spread. Moreover the results shows that this delay spread effect is independent of the shape of power delay profile as depicted in Figure 2.14. In [25] the effect of delay spread on the performance of OFDM based WLAN system has been investigated. The results show that with larger delay spread the SNR needed to achieve certain average packet error rate is decreased as depicted in Figure 2.15.

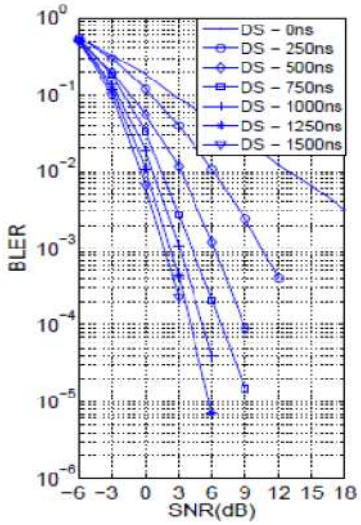

Figure 2.12 BLER in LTE system with different DSs. The system bandwidth is 1.4 MHz, no HARQ transmission, CQI = 1

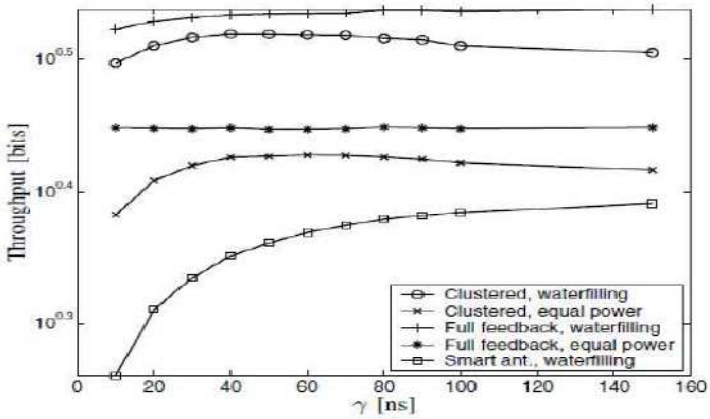

Figure 2.13 The effect of delay spread (γ) on the estimated throughput of OFDM system with different scheduling and power allocation methods. The number of users is 32 and the SNR is 32 dB

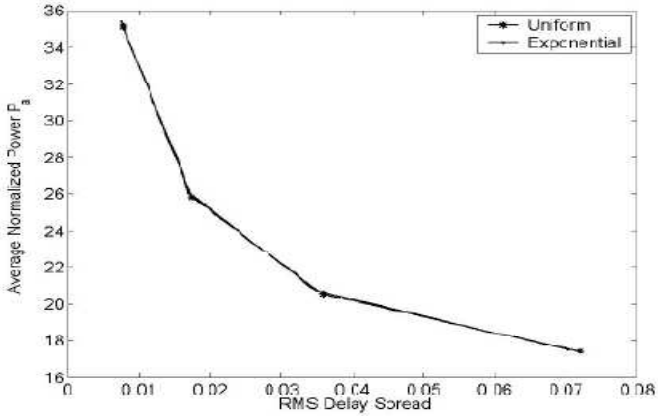

Figure 2.14 Average normalized power as a function of RMS delay spread under exponential and uniform power delay profile for OFDM system with 16QAM modulation

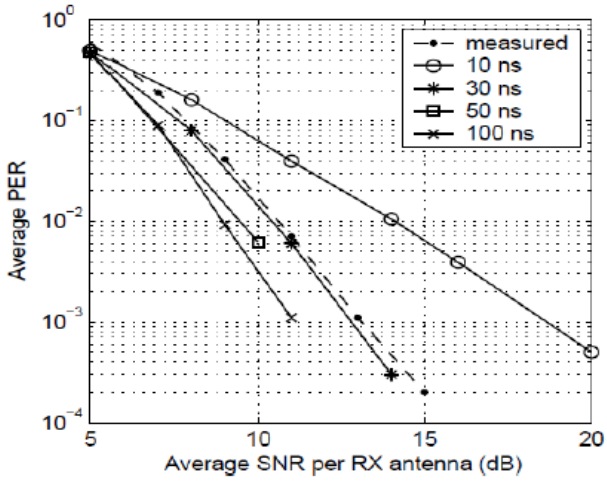

Figure 2.15 The effect of delay spread on the performance of OFDM based WLAN system

2.4.5 Angular Spread

Angular spread is variations in Angle of Arrival or Angle of Departure of different multipath components which arrive at the receiver or depart from the transmitter. Angular spread varies between locations and is usually larger at the mobile terminal than at the base station. According to a measurement conducted by TU Eindhoven in the vicinity of Amsterdam Arena, the observed angular spread varies from 20 degree up to 100 degree [21].

The quantification of angular spread is not as simple as for delay spread. In [27] the definition of circular angular spread is given. For a signal with N multi-paths, each with M subpaths, the angular spread calculation for the signal is given by:

$$\sigma_{AS} = \sqrt{\frac{\sum_{n=1}^{N}\sum_{m=1}^{M}\left(\theta_{n,m,\mu}{}^{2}\right)\cdot P_{n,m}}{\sum_{n=1}^{N}\sum_{m=1}^{M}P_{n,}}} \tag{2.13}$$

Where $P_{n,m} = P_n/20$ is the power of the m[th] subpath of the n[th] path, $\theta_{n,m,\mu}$ is defined as

$$\theta_{n,m,\mu} = \begin{Bmatrix} 2\pi + \left(\theta_{n,m} - \mu_\theta\right) & if\ \left(\theta_{n,m} - \mu_\theta\right) < -\pi \\ \left(\theta_{n,m} - \mu_\theta\right) & if\ \left|\theta_{n,m} - \mu_\theta\right| < \pi \\ 2\pi - \left(\theta_{n,m} - \mu_\theta\right) & if\ \left(\theta_{n,m} - \mu_\theta\right) > \pi \end{Bmatrix}$$

μ_θ is defined as

$$\mu_\theta = \frac{\sum_{n=1}^{N}\sum_{m=1}^{M}\theta_{n,m}\cdot P_{n,m}}{\sum_{n=1}^{N}\sum_{m=1}^{M}P_{n,m}}$$

and $\theta_{n,m}$ is the AoA or AoD of the m^{th} subpath of the n^{th} path.

Angular spread affects MIMO Performance

The relation between angular spread and MIMO performance is explained by the concept of spatial correlation. Angular spread determines coherence distance which is the minimum distance over which two antenna elements uncorrelated. Together with antenna spacing angular spread determines the spatial correlation between channel elements. When antenna spacing is larger than coherence distance, the spatial correlation between channel elements is small and the spatial diversity is obtained. The spatial correlation affects MIMO performance. Less spatial correlation between channel elements implies better MIMO performance.

Spatial correlation measures the dependency among antenna elements. Higher spatial correlation means higher dependency which means higher interference between signals transmitted or received by antenna elements. This results in degraded MIMO performance. Scattering decreases spatial correlation, and thus leads to more uncorrelated channel elements. At the same time scattering leads to increase of angular spread. Therefore it can be expected that the increase of angular spread results in improved MIMO performance.

The investigation on spatial correlation function of Spatial Channel Model (SCM) with different angular spread has been done in [8]. Figure 2.16 shows the spatial correlation of the signals at per path level which indicates that:

- When antenna spacing is larger than certain value (coherence distance), the spatial correlation is very small
- The coherence distance depends on the angular spread. The larger the angular spread, the smaller the coherence distance
- For a given antenna spacing, the spatial correlation is smaller for larger angular spread.

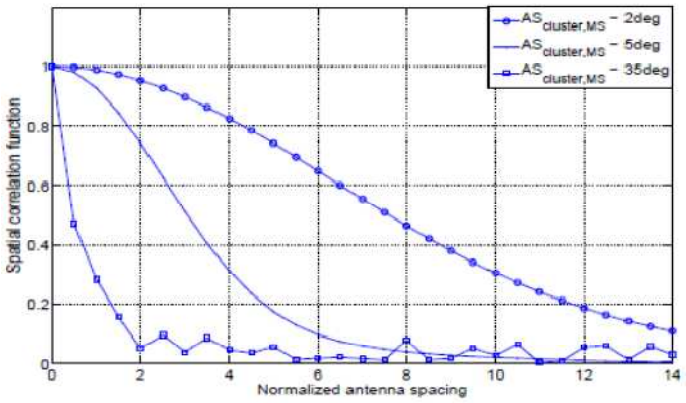

Figure 2.16 Path (cluster) level spatial correlation function versus normalized antenna spacing, the mean AoA is 60 degrees

In [26] the effect of angular spread on the capacity of MIMO performance has been investigated. The results show that the system capacity increases as angular spread increases. This result is depicted in Figure 2.17.

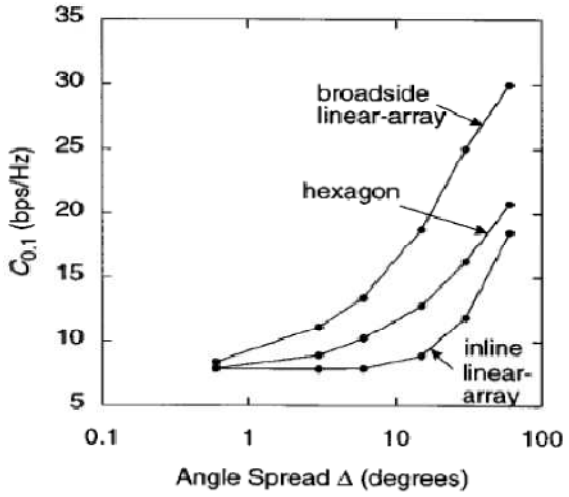

Figure 2.17 Channel capacity for hexagonal MIMO antenna system at various angular spread

2.4.6 MIMO Spatial Channel Model

Spatial Channel Model (SCM) is a 3GPP standard channel model for multi antenna system level simulation. In this model, the received signal is assumed to consist of N time-delayed multipath replicas and each of these N paths consists of M subpaths. Each of the N paths arrives at the receiver with different angle of arrival and time delay. Meanwhile each of the M subpaths of the n^{th} path arrives at the receiver with different angle of arrival but with the same time delay. In this research, downlink data transmission where a Base Station (BS) transmits to a Mobile Station (MS) is considered. The angular parameters of spatial channel model for downlink data transmission are depicted in Figure 2.18 and the description of these angular parameters is given in Table 2.8.

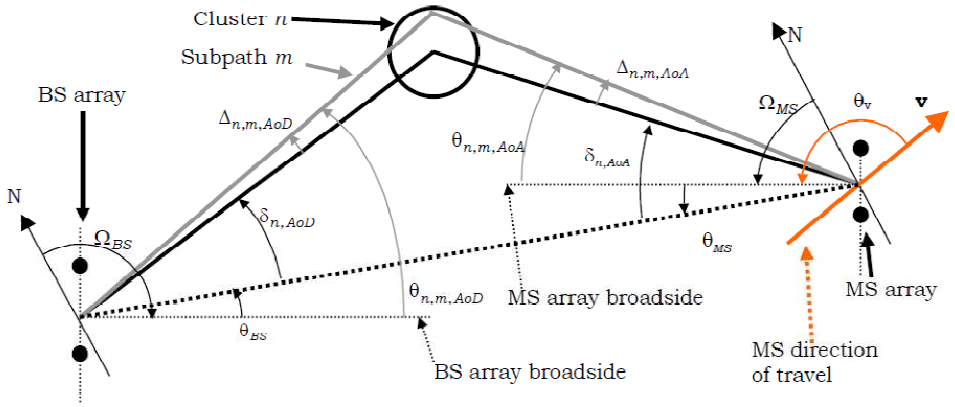

Figure 2.18 Angular parameters of spatial channel model in downlink direction [27]

Suppose there are S BS antenna elements and U MS antenna elements, the channel coefficients of one of N multipath components are given by a S x U matrix with complex amplitude. The channel impulse response of the nth multipath component between the uth transmit antenna and sth receive antenna is given by [27]

$$h_{u,s,n}(t) = \sqrt{\frac{P_n \sigma_{SF}}{M}} \sum_{m=1}^{M} \left(\sqrt{\begin{array}{c} G_{BS}(\theta_{n,m,AoD}) \exp\left(j\left[kd_s \sin(\theta_{n,m,AoD}) + \Phi_{n,m}\right]\right) \times \\ \sqrt{G_{MS}(\theta_{n,m,AoA})} \exp\left(jkd_u \sin(\theta_{n,m,AoA})\right) \times \\ \exp\left(jk\|v\| \cos(\theta_{n,m,AoA} - \theta_v)t\right) \end{array}} \right) \quad (2.14)$$

where P_n is the power of the nth path, σ_{sf} is the lognormal shadow fading, M is the number of subpaths per path, $G_{BS}(\theta_{n,m,AoD})$ is the BS antenna gain of each array element, $G_{MS}(\theta_{n,m,AoA})$ is the MS antenna gain of each array element, j is the square root of -1, k is the wave number $2\pi/\lambda$, where λ is the carrier wavelength in meters, d_s is the distance in meters between BS antenna element s and the reference (s=1) antenna. For the reference antenna s = 1, $d_1 = 0$. d_u is the distance in meters between MS antenna element u and the reference (u=1) antenna. For the reference antenna u =1, $d_1 = 0$. And $\Phi_{n,m}$ is the phase of the mth subpath of the nth path.

Table 2.8 Description of angular parameters in SCM [27]

Angular Parameter	Description
Ω_{BS}	BS antenna array orientation, defined as the difference between the broadside of the BS array and the absolute North (N) direction
Ω_{BS}	LOS AoD direction between the BS and MS with respect to the broadside of the BS array
$\delta_{n,AoD}$	AoD for the nth (n=1….N) path with respect to the LOS AoD θ_0
$\Delta_{n,m,AoD}$	Offset for the mth (m=1…M) subpath of the nth path with respect to $\delta_{n,AoD}$
$\theta_{n,m,AoD}$	Absolute AoD for the mth (m=1….M) subpath of the nth path with respect to the BS broadside
Ω_{MS}	MS antenna array orientation, defined as the difference between the broadside of the MS array and the absolute North reference direction
θ_{MS}	Angle between the BS-MS LOS and the MS broadside
$\delta_{n,AoA}$	AoA for the nth (n=1…N) path with respect to the LOS AoA $\theta_{0,MS}$
$\Delta_{n,m,AoA}$	Offset for the mth (m=1…M) subpath of the nth path with respect to $\delta_{n,AoA}$
$\theta_{n,m,AoA}$	Absolute AoA for the mth (m=1…M) subpath of the nth path at the MS with respect to the BS broadside
v	Velocity vector
θ_v	Angle of the velocity vector with respect to the MS broadside, $\theta_v = \arg(v)$

There are three different environments specified in SCM, namely urban macrocell, suburban macrocell and urban microcell. Macrocell has inter-site distance of 3 km, whereas that of microcell is about 1 km. Macrocell environment assumes that BS antennas are above roof top

height. While for microcell scenario, the BS antenna is at the rooftop height. Table 2.9 provides the parameters for these environments.

Table 2.9 Environment parameters in SCM [27]

Channel Scenario	Suburban Macro	Urban Macro	Urban Micro
Number of paths (N)	6	6	6
Number of sub-paths (M) per-path	20	20	20
Mean AS at BS AS at BS as a lognormal RV $\sigma_{AS} = 10\text{^}(\varepsilon_{AS}x + \mu_{AS})$, $x \sim \eta(0,1)$	$E(\sigma_{AS}) = 5^0$ $\mu_{AS} = 0.69$ $\varepsilon_{AS} = 0.13$	$E(\sigma_{AS}) = 8^0, 15^0$ 8^0 $\mu_{AS} = 0.810$ $\varepsilon_{AS} = 0.34$ 15^0 $\mu_{AS} = 1.18$ $\varepsilon_{AS} = 0.210$	NLOS: $E(\sigma_{AS}) = 19^0$ N/A
$r_{AS} = \sigma_{AOD}/\sigma_{AS}$	1.2	1.3	N/A
Per-path AS at BS (fixed)	2 deg	2 deg	5 deg (LOS and NLOS)
BS per-path AoD distribution standard distribution	$\eta(0, \sigma_{AoD}^2)$ where $\sigma_{AOD} = r_{AS}\sigma_{AS}$	$\eta(0, \sigma_{AoD}^2)$ where $\sigma_{AOD} = r_{AS}\sigma_{AS}$	U(-40deg, 40deg)
Mean AS at MS	$E(\sigma_{AS,MS}) = 68^0$	$E(\sigma_{AS,MS}) = 68^0$	$E(\sigma_{AS,MS}) = 68^0$
Per-path AS at MS (fixed)	35^0	35^0	35^0
MS per-path AOA Distribution	$\eta\left(0, \sigma_{AoA}^2\ (P_r)\right)$	$\eta\left(0, \sigma_{AoA}^2\ (P_r)\right)$	$\eta\left(0, \sigma_{AoA}^2\ (P_r)\right)$
Delay spread as lognormal RV $\sigma_{DS} = 10\text{^}(\varepsilon_{DS}x + \mu_{DS})$, $x \sim \eta(0,1)$	$\mu_{DS} = -6.80$ $\varepsilon_{DS} = 0.288$	$\mu_{DS} = -6.18$ $\varepsilon_{DS} = 0.18$	N/A
Mean total RMS Delay Spread	$E(\sigma_{DS}) = 0.17\ \mu s$	$E(\sigma_{DS}) = 0.65\ \mu s$	$E(\sigma_{DS}) = 0.251\ \mu s$
$r_{DS} = \sigma_{delay}/\sigma_{DS}$	1.4	1.7	N/A
Distribution for path delays			U(0, 1.2μs)
Lognormal shadowing standard deviation	8 dB	8 dB	NLOS: 10 dB LOS: 4 dB
Path loss model (dB), d is in meters	$31.5 + 35\log_{10}(d)$	$34.5 + 35\log_{10}(d)$	NLOS: $34.53 + 38\log_{10}$ (d) LOS: $30.18 + 26*\log_{10}$ (d)

The performance of MIMO system under SCM has been investigated in [28]by taking into account the effect of the number of antennas and the inter element distance. The results show that the capacity of the MIMO system doesn't increase linearly with the number of antennas. This is due to SCM uses more realistic assumptions of the signal propagation environment. It is also observed that the capacity of urban microcell is higher than the capacity of suburban macrocell. This is partly due to higher angular spread in urban microcell which leads to lower spatial correlation and thus higher capacity.

Chapter 3
Approach

Studies on the dependencies of LTE performance on wideband channel properties have been done in [8] as mentioned in the previous chapter. The results clearly show that delay spread could improve OFDM performance, while angular spread could improve MIMO performance. But, this investigation was done by performing link level simulations. A link level simulation models the link between a base station and a mobile station. It models all data processing in physical layer such as modulation, coding, interleaving, scrambling, etc. in order to evaluate the performance of a certain radio access technology in terms of BLER or FER (Frame Error Rate).

LTE link level simulation assumes fixed modulation and coding scheme (MCS) regardless channel variations. When radio channel condition is good, the probability that the block is successful is relatively high whereas when the radio channel condition is bad due to deep fading, the fixed MCS leads to high block error probability. Therefore, in LTE link level simulation, BLER varies following channel variation but the gross throughput is kept fixed.

In reality Adaptive Modulation and Coding Scheme (AMC) is implemented in LTE. Favorable channel conditions leads to higher throughput since higher MCS is chosen. Meanwhile, in the bad channel condition lower MCS is selected which still holds a reasonable BLER target. So, it can be concluded that by implementing AMC throughput varies following channel variation and BLER varies between 0 and a pre-specified BLER target.

For radio planning purpose, disregarding AMC seems to be an oversimplification. By implementing AMC, for a given SINR, the highest possible modulation and coding scheme is chosen, so AMC ensures that a higher throughput can be achieved. Hence, in this study, investigation on the effect of wideband channel properties on LTE performance is done by performing a system level simulation where AMC which responds to channel variation can be modeled. In order to implement AMC system level simulation needs an accurate prediction of link level performance in terms of BLER. For this reason, AWGN link level simulation is required.

By considering the implementation of AMC as mentioned above, the approach taken in this study covers three main parts which are also depicted in the block diagram of Figure 3.1. The first part is LTE link level simulation in AWGN channel for various modulation and coding schemes and for certain range of SNR values. The result of this simulation is curves of LTE performance in terms of BLER for various modulation and coding schemes. The second part is modeling channel behavior in frequency and time domain based on Spatial Channel Model taking into account

delay spread and angular spread. Channel response for 10 MHz frequency bandwidth and duration of 20s is generated and often called channel traces. The third part is LTE system level simulation which uses channel traces and the curves obtained from AWGN link level simulation as inputs. Finally, LTE performance in terms of throughput is obtained from system level simulation. More detail explanations about these steps are given in the subsequent chapters.

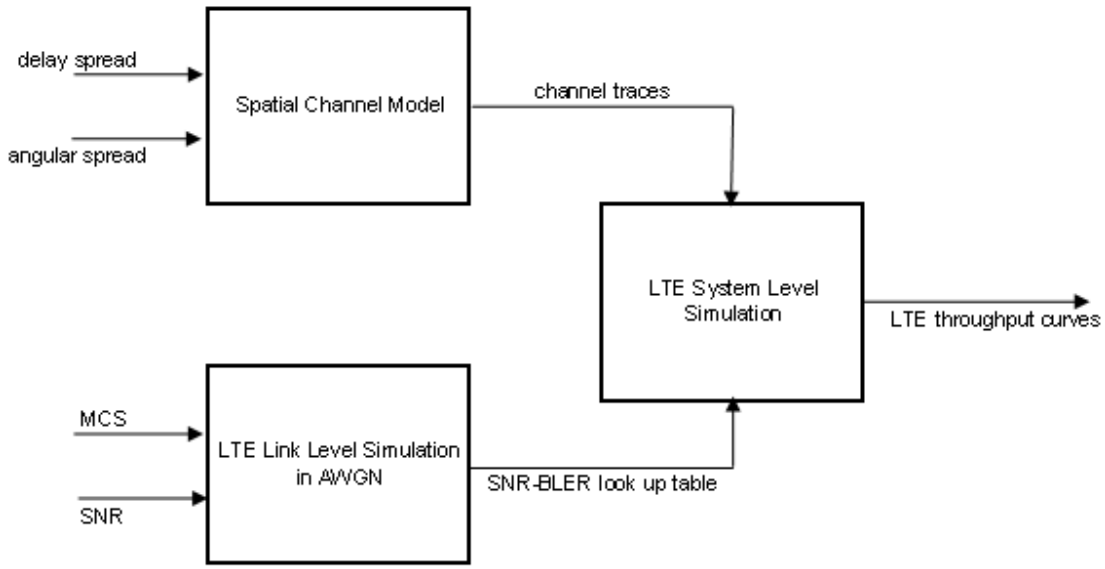

Figure 3.1 Block diagram of the approach taken in this study

Chapter 4
LTE System Level Simulation

The LTE system level simulation and its role in the overall approach have been briefly discussed in Chapter 3. This chapter discusses the process of LTE system level simulation in more detail. Section 4.1 provides a general overview of the system level simulation such as the network layout model, the propagation model, and the transmission modes. Section 4.2 describes the modeling of multipath channel behavior in the frequency and time domain according to SCM giving rise to the creation of channel traces. Finally, the link adaptation strategy in terms of Adaptive Modulation and Coding (AMC) based on AWGN link level simulation results is provided in section 4.3 together with the link to system mapping method based on EESM (Exponential Effective SINR Mapping).

4.1 Overview of LTE System Level Simulation

LTE system level simulations were performed by using a Delphi-based LTE system level simulator. The simulator models a network which consists of 12 cells. Further each cell is divided into 3 sectors. Only LTE downlink data transmission is simulated. One user in a random location is served by one base station and it experiences interference from other base stations. At any time, it is assumed that there is only one user served by BS and there is no coming request from other users.

Radio propagation model in the simulation counts the effect of path loss, shadowing and multipath fading. Some empirical path loss models are used such as Okumura Hata and COST 231 Hata model. The shadowing effect is modeled by Gaussian distribution with 0 mean and standard deviation of σ^2 in dB scale. Multipath fading effect is taken from separated simulation performed in Matlab and it follows a modified Spatial Channel Model (SCM) for MIMO simulation as will be explained in section 4.2.

Transmission Modes

Four transmission modes are implemented in the system level simulation namely SISO, Receiver Diversity (SIMO), MIMO Transmit Receive Diversity (MIMO TxRxD) and MIMO Spatial Multiplexing (MIMO SM). In SISO it is assumed that there is only one antenna at both transmitter and receiver. Meanwhile in SIMO, transmitter employs one antenna and receiver employs two antennas. In the receiver, the signals arrived at two different antennas are combined by assuming Maximal Ratio Combining (MRC). MIMO TxRxD and MIMO SM employ two antennas at both transmitter and receiver. The difference is that both transmit antennas in MIMO

TxRxD are used to transmit the same data stream expecting more robust received signals, while in MIMO SM both transmit antennas transmit different data stream expecting higher throughput at the receiver. Appendix A provides formulas to calculate instantaneous SINR in SIMO and MIMO modes.

TTI (Transmit Time Interval) based simulation flow

The simulation flow in each TTI consists of many processes. In the beginning of each TTI, the instantaneous complex channel response for each PRB is determined. Then instantaneous SINR per PRB is calculated hence there are 50 instantaneous SINRs. EESM (Exponential Effective SINR Mapping) is subsequently applied in order to get an effective SINR value from these SINRs. Once the effective SINR is obtained, the MCS (Modulation and Coding Scheme) which corresponds to a certain combination of modulation order and coding rate is determined. Subsequently, the block error rate for the effective SINR can be determined from the AWGN link level simulation results for the chosen modulation and coding scheme. If the block error rate is still lower than 10%, the process is repeated. A higher modulation and coding scheme can be selected and the BLER for the newly selected modulation and coding scheme can be determined again from AWGN link level simulation results. The iteration ends when the highest modulation and coding scheme which still meet the BLER requirement is obtained. Finally the data rate/throughput is calculated.

4.2 Channel Traces

Channel traces represent complex channel responses in time and frequency domain. In this study, multipath channel is modeled following Spatial Channel Model (SCM) for MIMO assuming 6 paths and 20 sub paths. However some modifications/simplifications were made in order to achieve the objectives of this study but with acceptable complexity (in the sense of computation time needed). Two main modifications are:

- Instead of assuming random delay spread as it is originally modeled in SCM, some fixed values according to 3GPP and ITU multipath channel models are assumed: Pedestrian A (PA), Pedestrian B (PB), Vehicular A (VA) and Typical Urban (TU) models. The combination of path powers and time delays in Pedestrian A corresponds to delay spread value of 45 ns, in Vehicular A to delay spread value of 370 ns, in Pedestrian B to delay spread value of 750 ns and in Typical Urban to delay spread value of 1000 ns.

- The mean angle of departure of the signal departing from the transmitter and mean angle of arrival of the signals arriving at the receiver are assumed to be fixed following the spatial correlation levels. There are three spatial correlation levels considered in this study, i.e. low, medium and high. Low correlation corresponds to spatial correlation of 0.19 at the BS and 0.22 at the MS side, medium correlation corresponds to spatial correlation of 0.32 at the BS and 0.79 at the MS, whereas high correlation corresponds to spatial correlation of 1 at the BS and 0.79 at the MS. The mean angle of arrival and mean

angle of departure are derived according to Figure 4.1 and Figure 4.2 for those spatial correlation values. Therefore low correlation is defined when the mean angle of arrival and mean angle of departure are 0 degree, medium correlation is defined when the mean angle of arrival is 90 degree and the mean angle of departure is 45 degree and finally high correlation is defined when the mean angle of arrival and mean angle of departure are both 90 degrees.

- Small scale fading, i.e. path loss and shadowing are calculated separately from SCM. They are calculated according to the propagation model defined in the system level simulation.

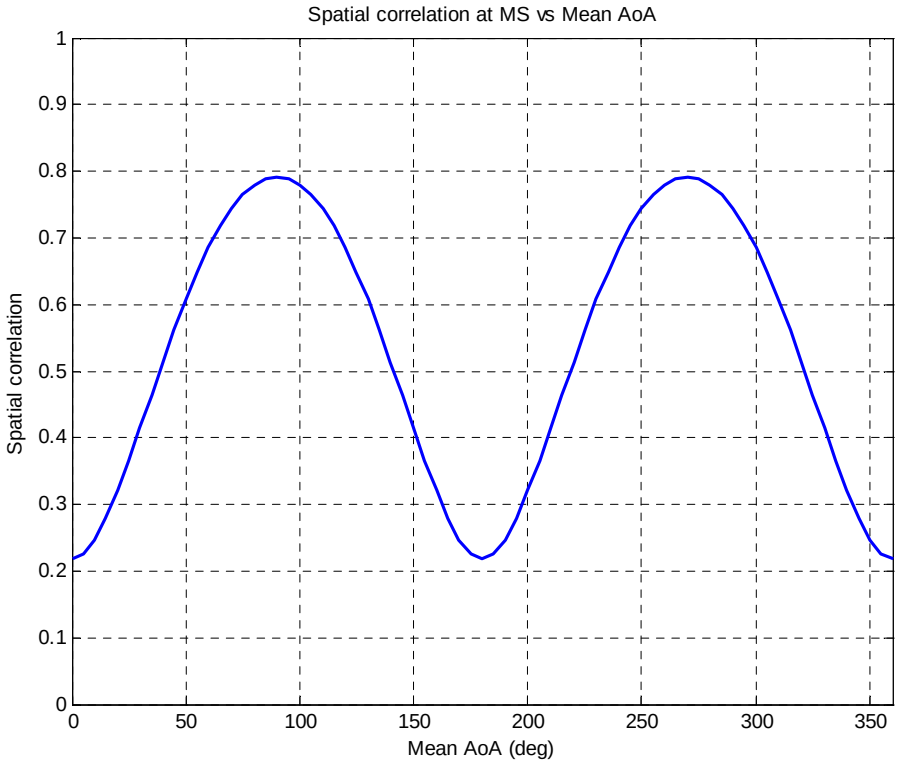

Figure 4.1 The relationship between mean Angle of Arrival and Spatial Correlation in SCM by assuming MS antenna spacing of 0.5 λ and BS antenna spacing of 10 λ

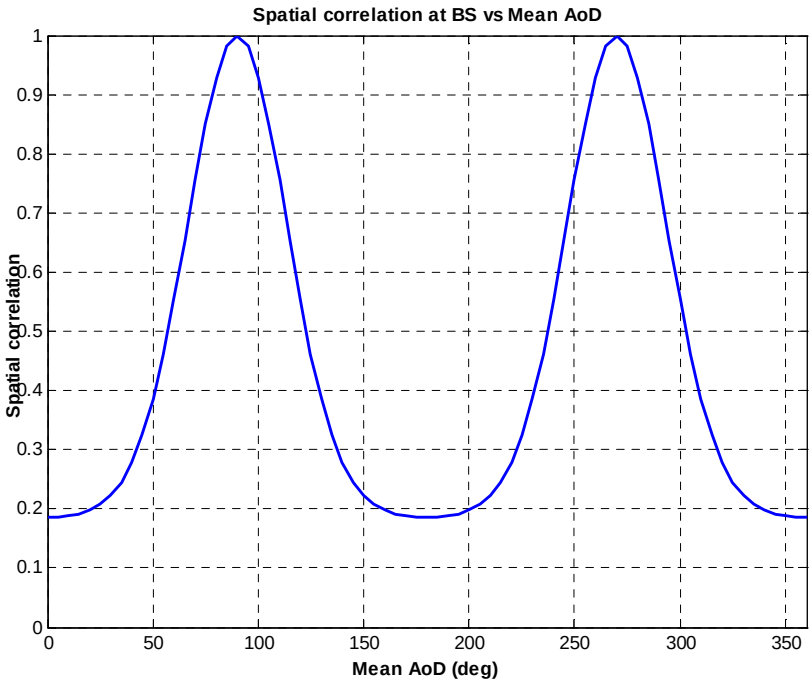

Figure 4.2 The relationship between mean Angle of Departure and Spatial Correlation in SCM by assuming MS antenna spacing of 0.5 λ and BS antenna spacing of 10 λ

The complete parameters used to generate channel traces in this study are given in Table 4.1.

Table 4.1 Parameters to generate channel traces

Parameters	Setting value
Number of antenna at BS	2
Number of antenna at MS	2
User velocity	3 km/h
Carrier frequency	2.6 GHz
Bandwidth	10 MHz
Environment	Urban Macrocell
Per path angular spread at BS	2 degree
Per path angular spread at MS	2, 5 or 35 degree
Delay spread	45, 370, 750 and 1000 ns
BS antenna spacing	10 lamda (λ)
MS antenna spacing	0.5 lamda (λ)

The magnitude of complex channel response or often called multipath fading gain obtained from the modified SCM are given in Figure 4.3, 4.4, 4.5, and 4.6 for Pedestrian A, Vehicular A, Pedestrian B, and Typical Urban respectively. Frequency domain fading gain is shown along the

X axis consisting of 50 PRBs where the channel response is assumed to be fixed within one PRB (180 kHz). The Y axis shows fading gain in time domain and it is represented in TTI (Transmit Time Interval) unit where one TTI lasts for 1 ms duration. The generated channel traces capture channel response for duration of at least 20000 TTI.

It can be observed from the figures that channel response of Pedestrian A is the most flat one in the frequency domain, while that of Typical Urban is the most varying one. This can be explained by the concept of coherence bandwidth. Coherence bandwidth is inversely proportional to delay spread, i.e. when the delay spread is larger the coherence bandwidth is smaller, and vice versa. Pedestrian A has the lowest delay spread value, so the coherence bandwidth in Pedestrian A is the largest. It means that the frequency range over which flat channel response occurs is larger in Pedestrian A compared to other multipath propagation models. On the other hand, Typical Urban has the largest delay spread value which results in smallest coherence bandwidth among other multipath propagation models. Hence, the frequency domain channel response is the most varying.

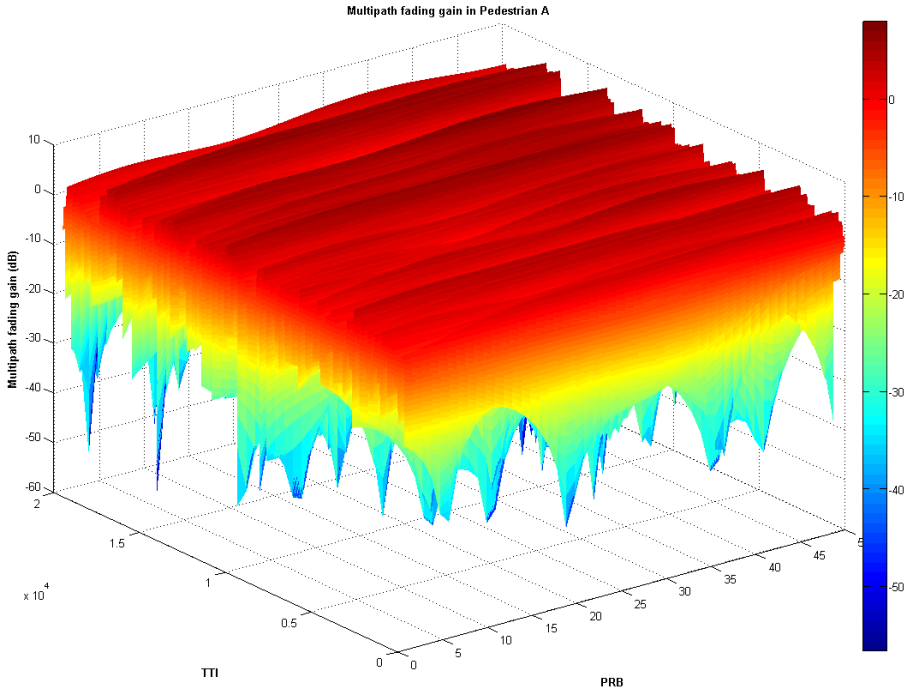

Figure 4.3 Multipath fading gain in time and frequency domain of Pedestrian A

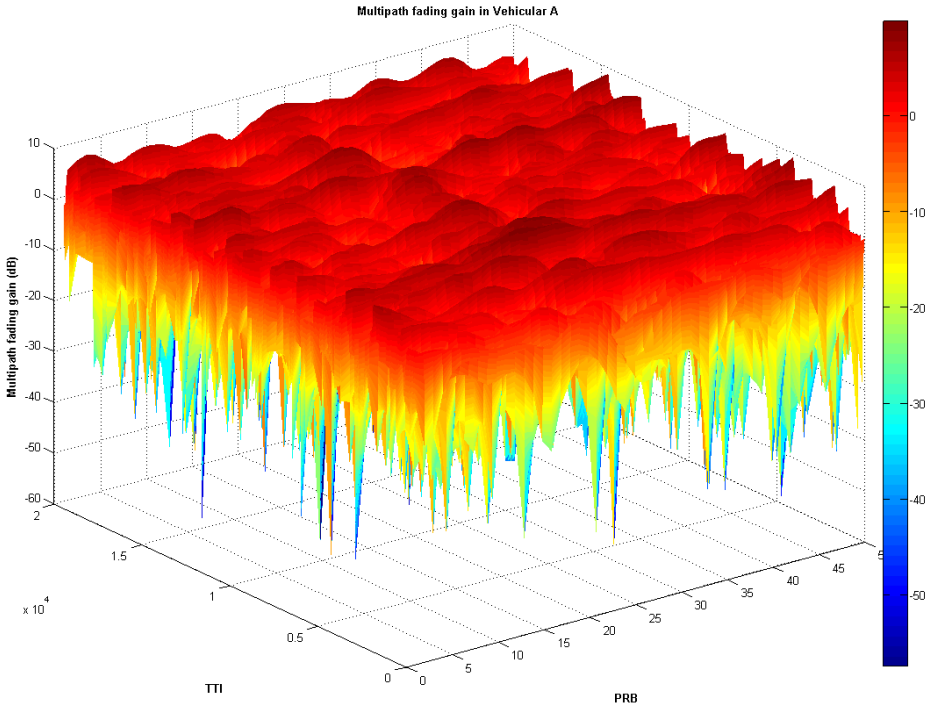

Figure 4.4 Multipath fading gain in time and frequency domain of Vehicular A

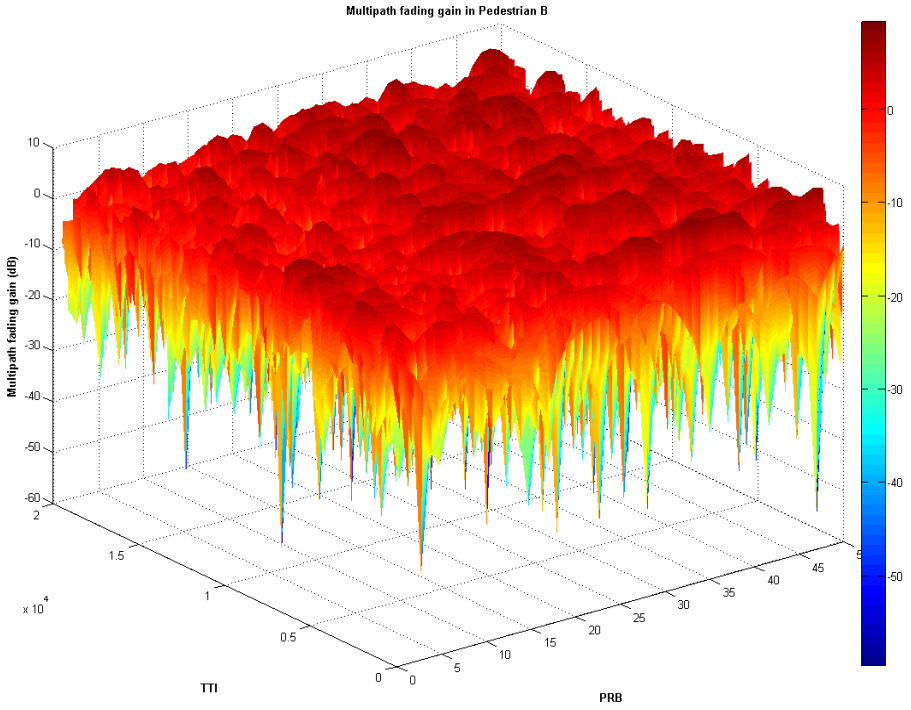

Figure 4.5 Multipath fading gain in time and frequency domain of Pedestrian B

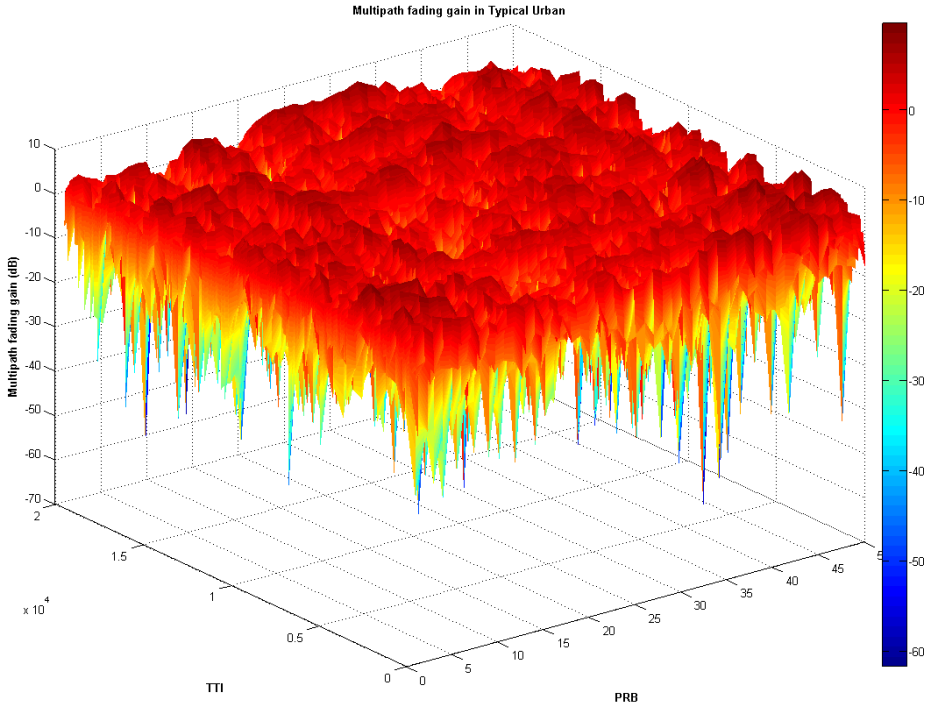

Figure 4.6 Multipath fading gain in time and frequency domain of Typical Urban

In this study, two antennas are employed at both the transmitter and the receiver namely Tx_1, Tx_2 and Rx_1, Rx_2 as shown in Figure 4.7. There are four pairs of transmit and receive antennas, i.e. transmit antenna one receive antenna one (Tx_1Rx_1), transmit antenna one receive antenna two (Tx_1Rx_2), transmit antenna two receive antenna one and transmit antenna two receive antenna two (Tx_2Rx_2). The medium between each pair of antennas corresponds to a distinct wireless channel. Hence, the signal transmitted and received in each pair of antennas experience different channel response.

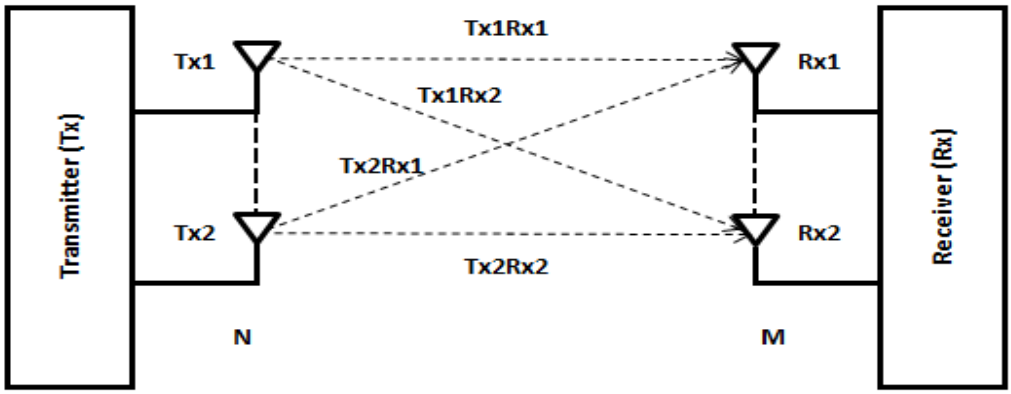

Figure 4.7 2x2 MIMO System

The spatial correlations between two transmit antennas and two receive antennas affect the independency of the channel response of each transmit receive antenna pair. If the spatial correlations between two transmit antennas and between two receive antennas are high, the signal transmitted and received in different pair of antennas experience correlated fading. On the other hand, if the correlations between two transmit antennas and between two receive antennas are low, the signal transmitted and received in different pair of antennas experience independent fading. This can be seen from the channel traces shown in Figure 4.8, 4.9 and 4.10 for Pedestrian A with low, medium and high correlation respectively. The red curve shows multipath fading gain for antenna pair Tx_1Rx_1, the green color shows multipath fading gain for antenna pair Tx_1Rx_2, the blue curve shows multipath fading gain for antenna pair Tx_2Rx_1 and the yellow curve shows multipath fading gain for antenna pair Tx_2Rx_2. The figures show that in the case of low correlation between both transmit antennas and receive antennas, multipath fading gains are independent each other, in the case of high correlation, multipath fading gains are correlated, whereas in the case of medium correlation, the independencies among multipath fading gains are in between those for low and high correlation.

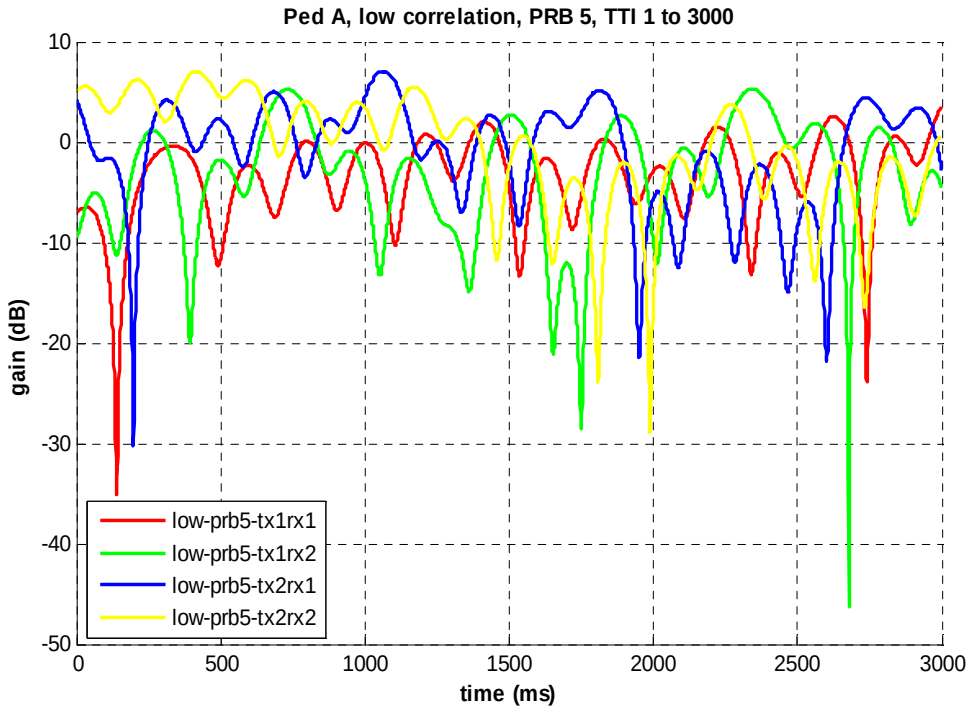

Figure 4.8 Multipath fading gain in Pedestrian A with Low Correlation

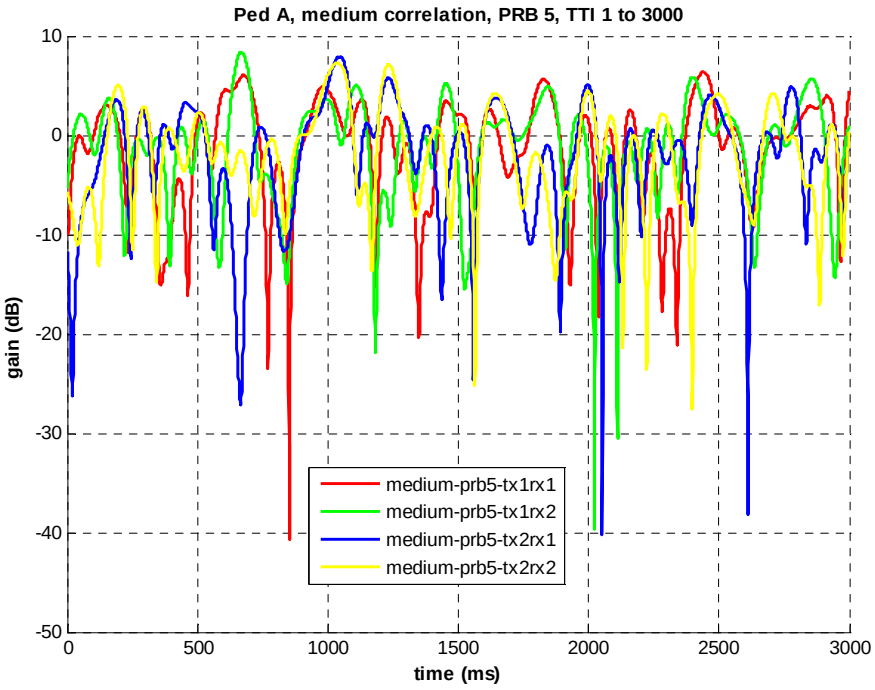

Figure 4.9 Multipath fading gain in Pedestrian A with Medium Correlation

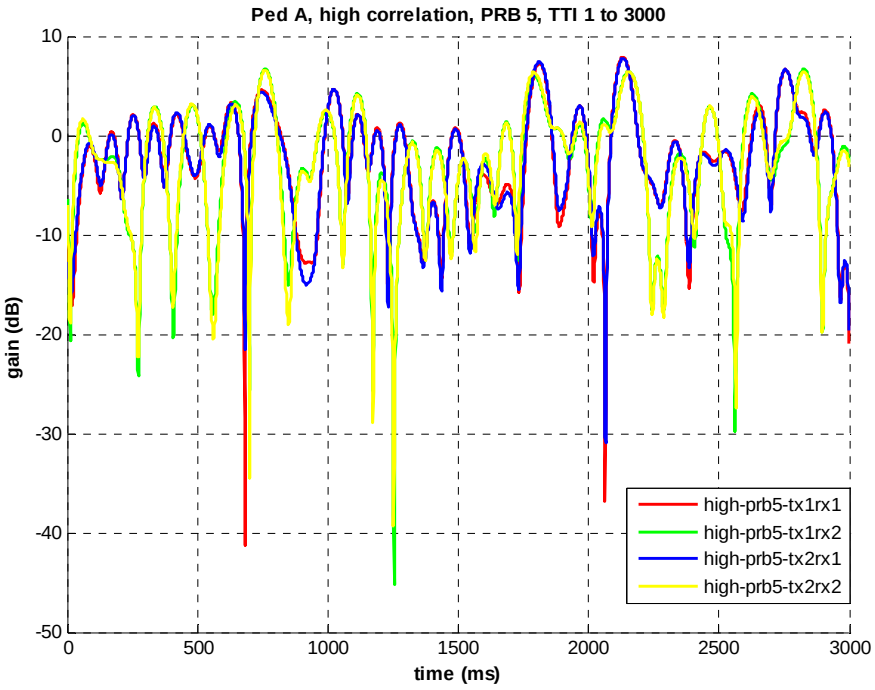

Figure 4.10 Multipath fading gain in Pedestrian A with High Correlation

Another wideband channel property investigated in this study is angular spread. In SCM two angular spreads are defined, namely (overall) angular spread and per-path angular spread. Angular spread describes the variations of angle of arrival or angle of departure of different paths and is assumed to be random variable following lognormal distribution. While per-path angular spread describes the variations of angle of arrival or angle of departure of different sub-paths within one path. Only per-path angular spread at the MS are considered in this study assuming three different values, i.e. 2, 5 and 35 degree.

Figures 4.11, 4.12 and 4.13 depict multipath fading gains for antenna pair Tx_1Rx_1 and Tx_1Rx_2 for per path angular spread of 2, 5 and 35 degree respectively. Only Tx_1Rx_1 and Tx_1Rx_2 are considered since three different per path angular spread values at the mobile station are investigated. Therefore, there is no impact of these angular spread values on the spatial correlation at the BS side. From those figures it can be seen that multipath fading gain for antenna Tx_1Rx_1 and Tx_1Rx_2 are highly correlated for per path angular spread of 2 and 5 degree but for per path angular spread of 35 degree they are less correlated. The spatial correlations for per path angular spread of 2 and 5 degree are 0.32 at the BS and 1 at the MS, whereas the spatial correlations for per path angular spread of 35 degree are 0.32 at the BS and 0.79 at the MS. This phenomenon can be explained by the principle of coherence distance. Angular spread is inversely proportional to coherence distance, i.e. larger angular spread results in lower coherence distance and vice versa. Thus, per path angular spread of 35 degree has lower coherence distance compared to per path angular spread of 2 and 5 degree. Therefore the channel responses in Tx_1Rx_1 and Tx_1Rx_2 for per path angular spread of 35 degree are less correlated compared to those of per path angular spread of 2 and 5 degree. Meanwhile, in the case of angular spread of 2 and 5 degree, the coherence distance are larger than those of 35 degree, hence the channel responses in Tx_1Rx_1 and Tx_1Rx_2 for per path angular spread of 2 and 5 degree are highly correlated as shown in Figure 4.11 and 4.12.

4.3 Link Adaptation

One of the key features of LTE is the implementation of link adaptation [30]. Link adaptation aims at matching the data rate for each user according to the variations in received signal quality. The LTE system level simulation performed in this study implements link adaptation based on Adaptive Modulation and Coding (AMC). AMC works as follows: based on the received SINR, modulation and coding scheme is chosen in such a way that the user data rate is maximized while at the same time the block error rate is not more than 10% (tunable). The selection of modulation and coding scheme is done on TTI basis. Thus, every 1 ms the modulation and coding scheme might be adjusted.

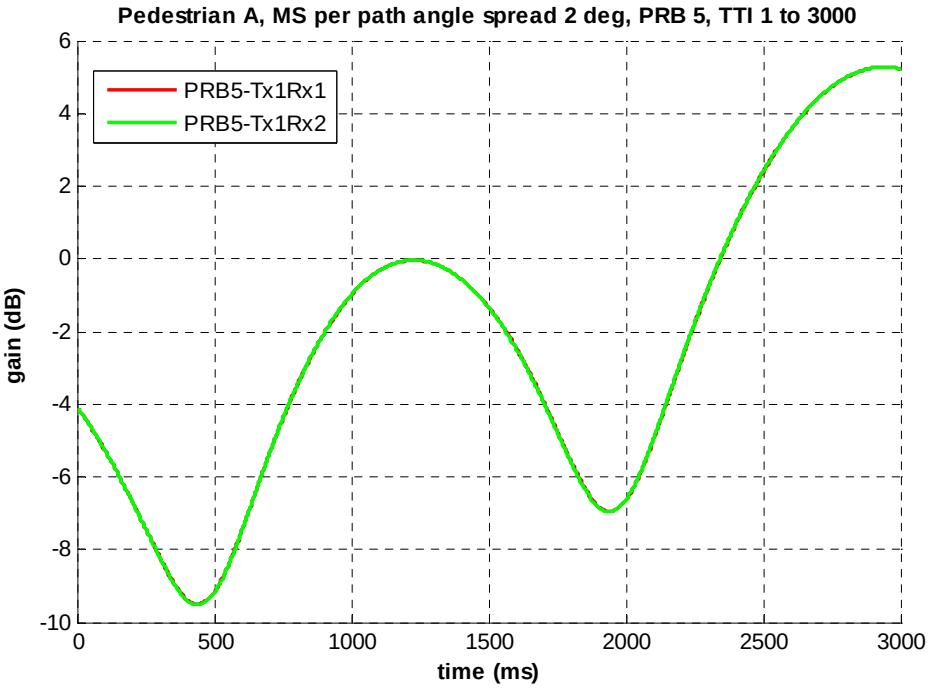

Figure 4.11 Multipath fading gain in Tx1Rx1 and Tx1 Rx2 for Pedestrian A with per path angular spread 2°

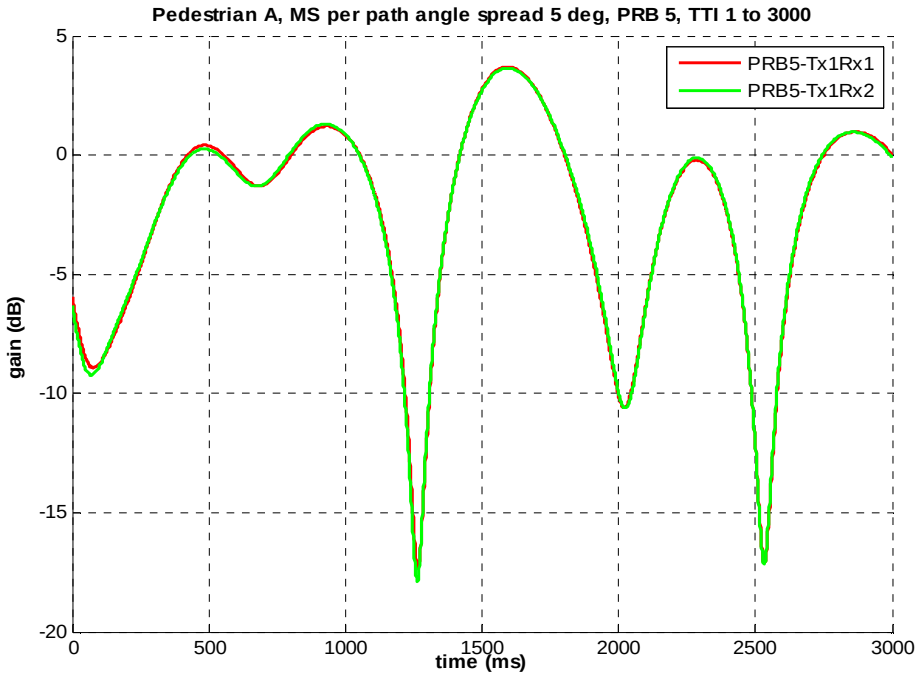

Figure 4.12 Multipath fading gain in Tx1Rx1 and Tx1Rx2 for Pedestrian A with per path angular spread 5°

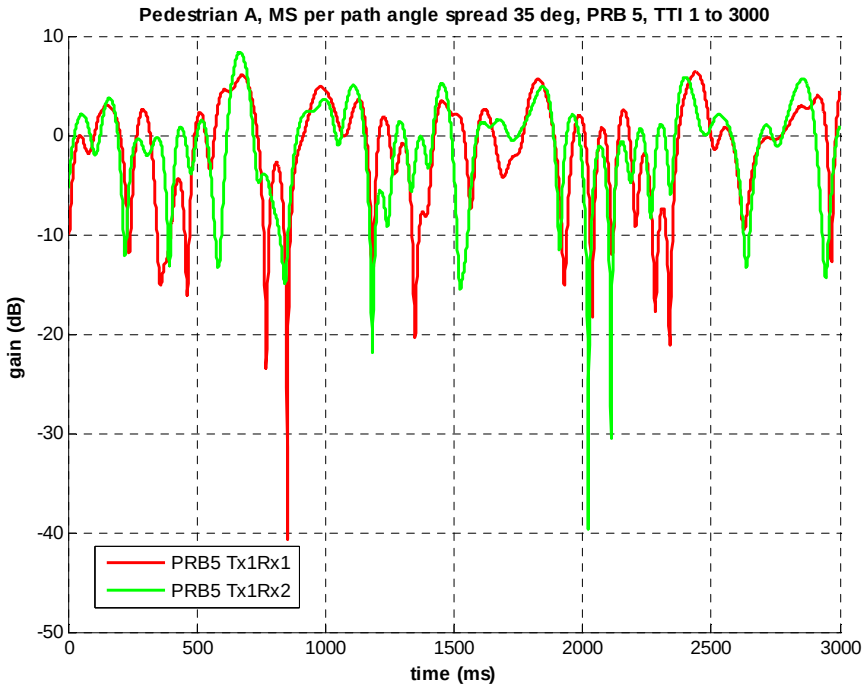

Figure 4.13 Multipath fading gain in Tx1Rx1 and Tx1Rx2 for Pedestrian A with per path angular spread 35 ^{o}

There are three modulation orders supported in LTE, namely QPSK, 16 QAM and 64 QAM. The complete modulation and coding schemes (MCS) are provided in Table 4.2. CQI index represents an indication of the data rate which can be supported by the channel taking into account the SINR and the characteristics of UE receiver. This CQI is in principle fed back by the UE to the BS and is used as an input for the selection of modulation and coding schemes. But in this study, CQI feedback is not modeled in the system level simulation due to its complexity.

The system bandwidth considered in this study is 10 MHz, thus the number of PRB is 50. The received signal power of each PRB may be different due to frequency selective fading yielding 50 different instantaneous SINRs over all PRBs. On the other hand, only single codeword (in the case of SISO) is employed over all the PRBs assigned to the UE. So, there should be a mechanism to bring these SINRs into one SINR value which is then used to determine the modulation and coding scheme of the codeword. In this study the mechanism is based on EESM (Exponential Effective SINR Mapping). The detail of EESM is explained in subsection 4.3.1.

Table 4.2 Combination of modulation scheme and coding rate in LTE [31]

CQI Index	Modulation	Approximate Code Rate	Efficiency (information bits per symbol)
0	No transmission	-	-
1	QPSK	0.076	0.1523
2	QPSK	0.12	0.2344
3	QPSK	0.19	0.3770
4	QPSK	0.3	0.6016
5	QPSK	0.44	0.8770
6	QPSK	0.59	1.1758
7	16 QAM	0.37	1.4766
8	16 QAM	0.48	1.9141
9	16 QAM	0.6	2.4063
10	64 QAM	0.45	2.7305
11	64 QAM	0.55	3.3223
12	64 QAM	0.65	3.9023
13	64 QAM	0.75	4.5234
14	64 QAM	0.85	5.1152
15	64 QAM	0.93	5.5547

4.3.1 Exponential Effective SINR Mapping (EESM)

Effective SINR Mapping (ESM) is a compression function of translating instantaneous channel state SINRs, PRB-specific SINRs in the case of LTE, into a single value, effective SINR, as shown in Figure 4.14. This effective SINR is then used to determine the modulation and coding schemes and estimate the block error probability according to link level performance in AWGN channel.

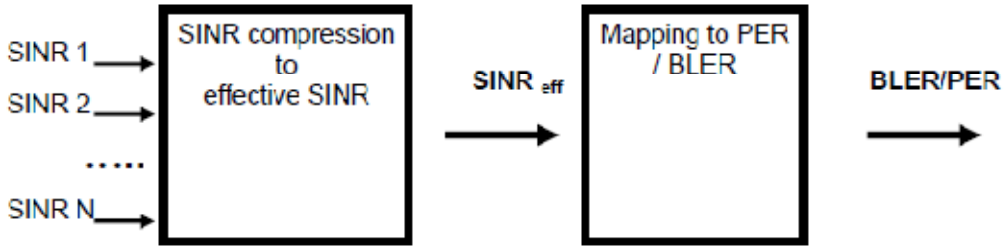

Figure 4.14 Principles of EESM

The basic AWGN link level performance in terms of BLER (Block Error Rate) used in this study is referring to [32]which have investigated LTE link level performance for 15 modulation and coding schemes (MCS) driven by 15 CQIs (channel quality indicator) as shown in Table 4.2. The results show that for higher modulation and coding scheme, in general the SINR required to achieve a specific BLER is higher. In other words, with the same SINR higher modulation order and coding rate results in higher block error rate. Thus, in the case of AMC, when the SINR is

high, a higher modulation and coding scheme can be selected as long as the BLER requirement is fulfilled. This results in higher achievable data rate while the BLER is still below the BLER target which in this study is set to 10%.

Exponential Effective SINR Mapping (EESM) is an effective SINR mapping method which assumes that all subcarriers (or PRBs in the case of LTE) for one radio terminal employ the same modulation and coding scheme. The effective SINR can be calculated as follows:

$$SINR_{eff} = -\beta \ln\left[\frac{1}{P}\sum_{p=1}^{P} \exp\left(-\frac{SINR_p}{\beta}\right)\right] \quad (4.1)$$

Where P is the number of subcarriers/PRBs, $SINR_P$ is the instantaneous SINR for PRB P and β is a parameter that in principle is obtained from calibration and is unique for each modulation and coding scheme. The set of beta values used in this study is given in Table 4.3 and is referring to those in [33] but an interpolation was done in order to get the more accurate beta value for each combination of modulation and coding scheme.

Table 4.3 Beta values used in the study [33]

MCS	Modulation	Coding rate	Beta
0	-	-	-999999999.99
1	QPSK	0.076	1.33
2	QPSK	0.12	1.33
3	QPSK	0.19	1.33
4	QPSK	0.3	1.33
5	QPSK	0.44	1.42
6	QPSK	0.59	1.6
7	16 QAM	0.37	3.8
8	16 QAM	0.48	4.8
9	16 QAM	0.6	6.1
10	64 QAM	0.45	10
11	64 QAM	0.55	15
12	64 QAM	0.65	19.3
13	64 QAM	0.75	25.8
14	64 QAM	0.85	31.3
15	64 QAM	0.93	35

Chapter 5
System Level Simulation Results

This chapter starts with Section 5.1 which provides parameter settings used in the LTE system level simulation performed in this study. Then Section 5.2 gives the simulation results together with the discussion on those results. Finally based on the simulation results, Section 5.3 provides recommendations for radio planning.

5.1 Parameter Settings

LTE system level simulations were done by assuming urban macrocell environment and considering four different delay spread values, three spatial correlation levels and two per path MS angular spread values as mentioned in the previous chapter. Within one simulation, the delay spread, the correlation level and the per path angular spread have equal values for the serving cell and all interfering cells. Moreover, beta values used by EESM are the same for all propagation models. Multipath channel model follows modified Spatial Channel Model. Path loss is calculated following COST 231 Hata model and shadowing is assumed to follow lognormal distribution with standard deviation of 8 dB. Four transmission modes are considered, namely SISO, SIMO (Receive Diversity), MIMO Transmit Receive Diversity and MIMO Spatial Multiplexing. During the whole simulation, 1000 users at different locations are simulated. But at any time, only one user is served. The service of each user lasts for duration of 30000 TTI or equals to 30 s.

5.2 System Level Simulation Results

This section provides the system level simulation results started with SISO simulation results to investigate the effect of delay spread. Then it is followed by SIMO and MIMO simulation results in order to analyse the effect of spatial correlation. And at last, the simulation result in MIMO to investigate the effect of angular spread is provided. The analysis of those simulation results is later used as bases for recommendations for radio planning. One terminology, SINR gain is introduced during the analysis. SINR gain is the difference in the required SINR between different delay spread values/spatial correlation levels/angular spread values in order to achieve the same LTE performance in terms of throughput.

5.2.1 SISO Results

SISO simulations were performed in order to investigate the effect of delay spread on LTE system performance. The original simulation result looks like the one depicted in Figure 5.1 which shows 1000 points corresponding to throughput in 1000 locations. The X axis corresponds to the SINR calculated by only considering large scale fading, i.e. path loss and shadowing. This SINR is later called average SINR. The Y axis shows the average throughput over 30000 TTIs. The simulation results show that throughput increases as the SINR increases and throughput of 10 Mbps is achieved at average SINR of about 8 dB. It is also observed that by performing the simulation over 30000 TTIs, fluctuations due to randomness in small scale fading are converged.

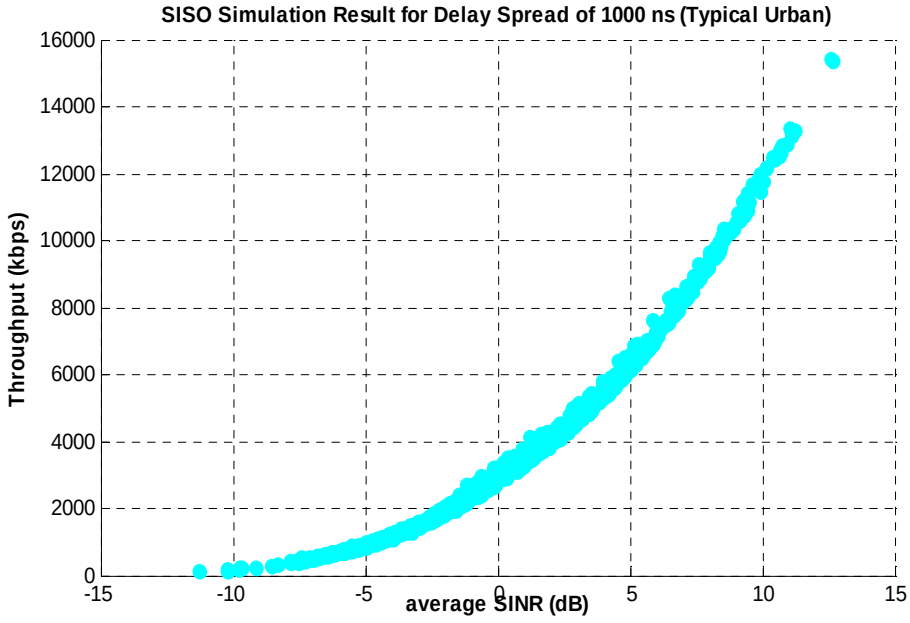

Figure 5.1 System level simulation result before data processing

All simulation results are further processed by calculating the average throughput of 1 dB range of average SINR thus resulting in smoother curves like the one depicted in Figure 5.2. Figure 5.2 shows SISO system level simulation result for average SINR from -11.5 till 12.5 dB. There are four curves correspond to delay spread value of 45 ns, 370 ns, 750 ns and 1000 ns respectively. As we can see, the result shows that different delay spread values do not significantly affect the system level performance of LTE. Table 5.1 shows the SINR gain obtained by using the curve of delay spread of 45 ns as the reference. To achieve throughput of 10 Mbps, the achieved SINR gains are 0.04 dB, 0.05 dB, and 0.31 dB for delay spread of 370 ns, 750 ns, and 1000 ns respectively. Since the SINR gains are small, it can be said that the SINR required to achieve the same throughput are almost same for all channels with different delay spread values. The almost same performance obtained from different delay spread values can be explained by exploring the detail information in each TTI.

Table 5.1 SINR gains obtained from different delay spread values

Throughput (Mbps)	SINR gain (dB)		
	DS = 370 ns	DS = 750 ns	DS = 1000 ns
4	0.19	0.09	-0.22
6	0.09	0.02	-0.36
8	0.06	0	-0.32
10	0.04	0.05	-0.31
12	0.03	-0.01	-0.31
14	-0.05	-0.07	-0.29

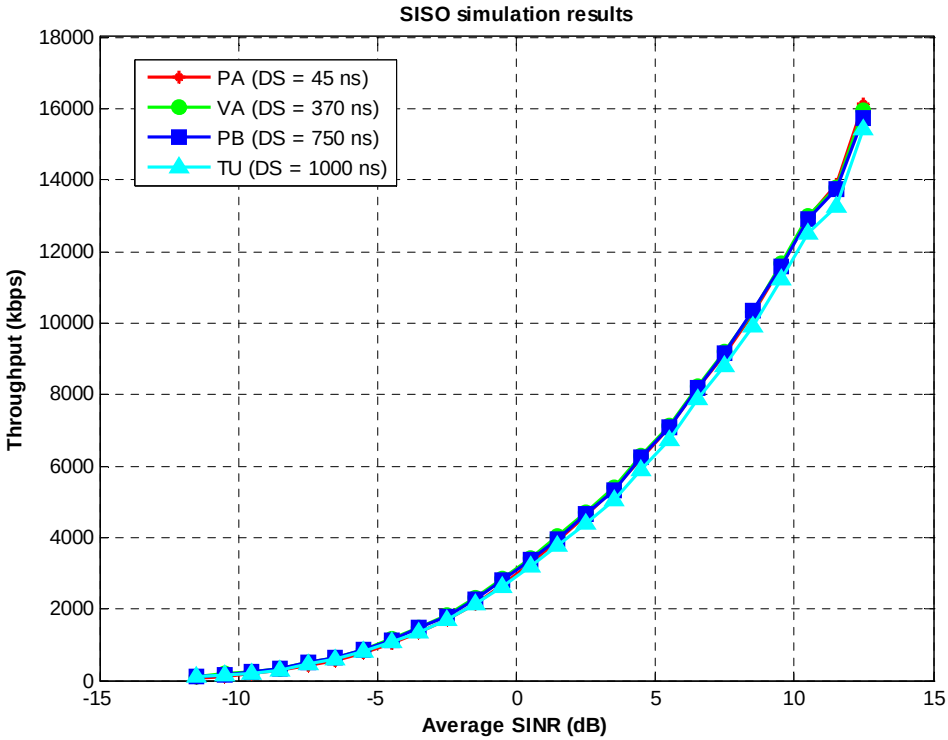

Figure 5.2 SISO simulation result

Detail information in TTI level

Figure 5.3 shows the variations of effective SINR for duration of 30 s. The red curve corresponds to the effective SINR for delay spread value of 45 ns, the green curve corresponds to the effective SINR for delay spread value of 370 ns, the dark blue curve corresponds to the effective SINR for delay spread value of 750 ns, and the light blue curve corresponds to delay spread value of 1000 ns. It can be observed from the figure that in some TTIs the effective SINR for low delay spread (e.g. the red curve) is higher than those for higher delay spread, but in some other TTIs lower than those for higher delay spread value. This is due to the fact that the channel frequency response is more flat for lower delay spread. Therefore, the neighbouring PRBs have high correlation in channel response. In some TTIs all PRBs may experience deep fading thus each

PRB has low SINR which then results in low effective SINR. In some other TTIs, all PRBs may be free from fading, so each PRB has high SINR which then results in high effective SINR. On the other hand, in the case of higher delay spread, the channel response is more frequency selective. Therefore the PRBs are less correlated. Some PRBs may suffer from deep fading, but some other PRBs experience good channel response. Consequently within one TTI, some PRBs have high instantaneous SINR but some PRBs have low instantaneous SINR. Thus the effective SINR is not so high but also not so low as shown in the green, dark blue and light blue curve.

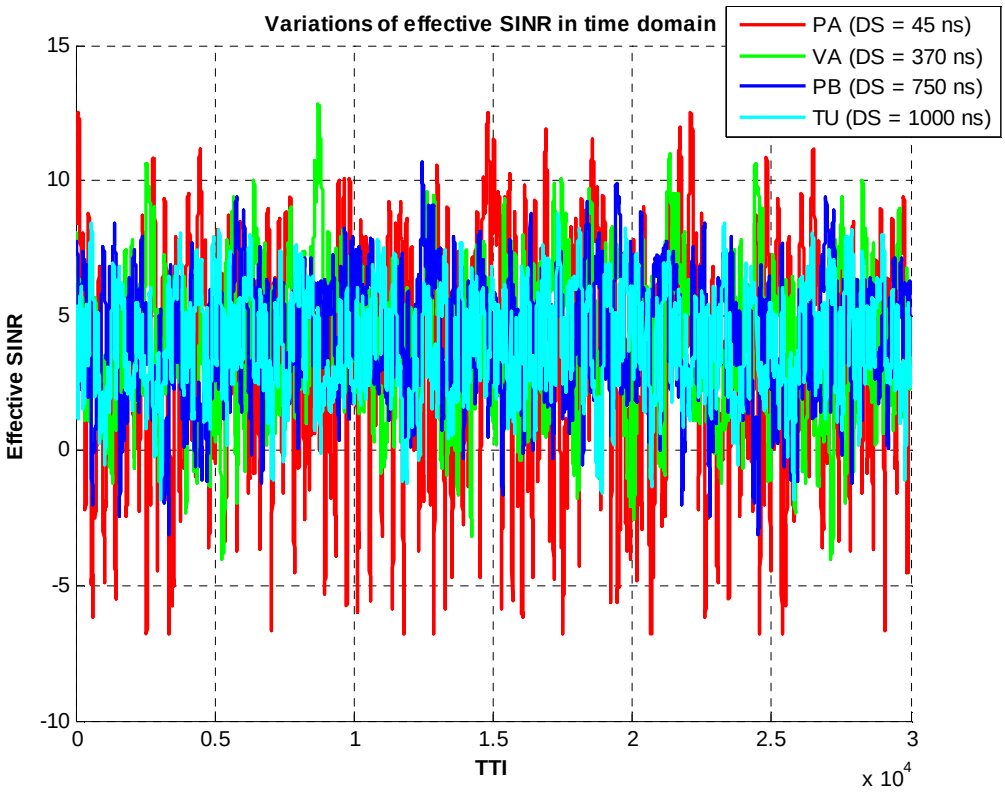

Figure 5.3 Variations of effective SINR in time domain

The effective SINR is used to determine the modulation and coding scheme (MCS). Thus the trend of effective SINR variations in time domain will also appear in the variations of chosen MCS as shown in Figure 5.4. It can be observed from both Figure 5.3 and Figure 5.4 that when the effective SINR is high the chosen MCS will be high. On the other hand, when the effective SINR is low, the chosen MCS will be low. It can also be seen that the lowest delay spread has the largest variations in the chosen MCS, because its effective SINR has the largest variation.

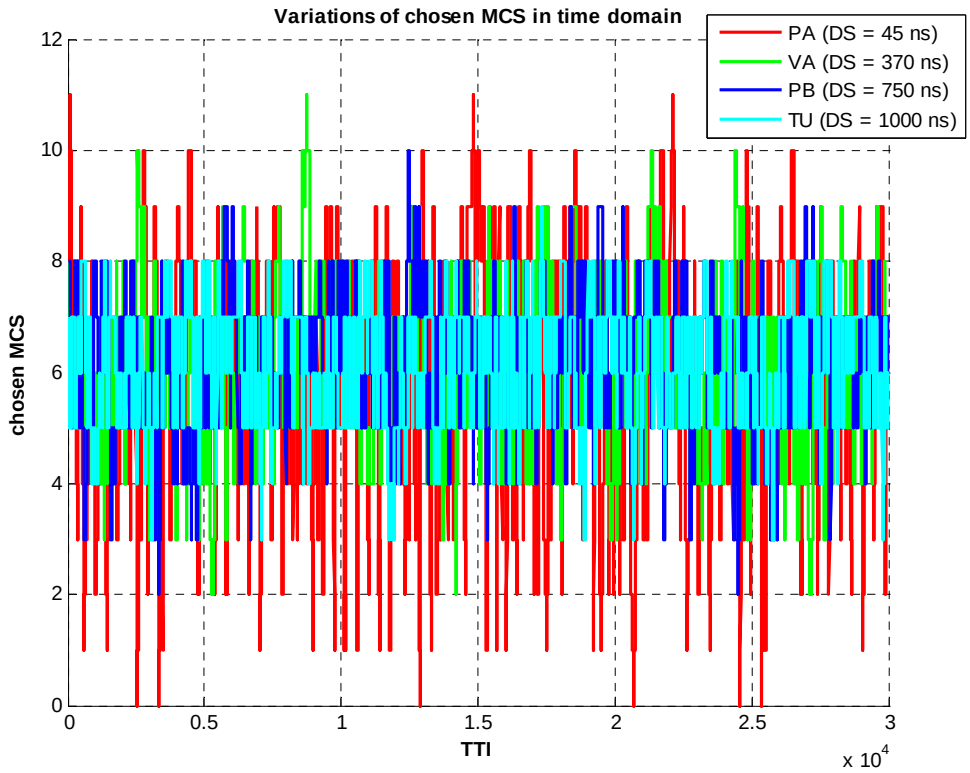

Figure 5.4 Variations of chosen MCS in time domain

The channel response in frequency domain can also be observed by exploring the number of PRBs assigned to each user. Due to deep fading, PRBs may have very low SINR, so the corresponding PRBs will be dropped. In other words, those PRBs will not be used to transmit any data. Consequently those PRBs do not contribute to the user throughput. The variations of number of PRBs assigned to the user are shown in Figure 5.5. It can be seen from the figure that for lower delay spread (e.g. red curve) sometimes all PRBs are assigned to the user but sometimes all PRBs are dropped due to deep fading. While for higher delay spread, sometimes all PRBs are assigned to the user but sometimes a few PRBs are dropped. In the channel with higher delay spread, all PRBs being dropped doesn't occur since PRBs are less or not correlated thus there are always PRBs with high SINR and there are always PRBs with low SINR.

The number of assigned PRBs per TTI and the chosen MCS together determine the throughput that the user can get per TTI. The variations of throughput in time domain for all delay spread values are shown in Figure 5.6. It can be seen that the range of throughput variation in delay spread of 45 ns is the highest, the range of throughput variation in delay spread of 1000 ns is the lowest, and the range of throughput variation in delay spread of 370 ns and 750 ns is in between. This happens because for delay spread of 45 ns when it experiences deep fading, all the PRBs are dropped, thus there are no PRBs used to transmit the data. Consequently throughput is zero. But, when the PRBs are in good condition, all PRBs are assigned. Moreover those PRBs have high

effective SINR which leads to high chosen MCS. Hence, the throughput becomes very high. On the other hand, in the case of other delay spread values, even though all the PRBs are assigned to the user but the effective SINR of those PRBs are not as high as the peak effective SINR in the delay spread of 45 ns. Thus resulted throughput is not as high as in delay spread of 45 ns.

By observing throughput variations for all delay spread values as shown in Figure 5.6 it can be concluded that the range of throughput variations in time domain is inversely proportional to the delay spread value. But after averaging out the variations over 30000 TTIs, the average throughput will be almost the same as shown Figure 5.1. The high throughputs in some TTIs achieved by low delay spread compensate the low throughput in some other TTIs. The “not so high” throughput achieved by higher delay spread in some TTIs compensate the “not so low” throughput in some other TTIs. That might explain why no significant difference is observed in the average throughput (averaged over 30000 TTIs).

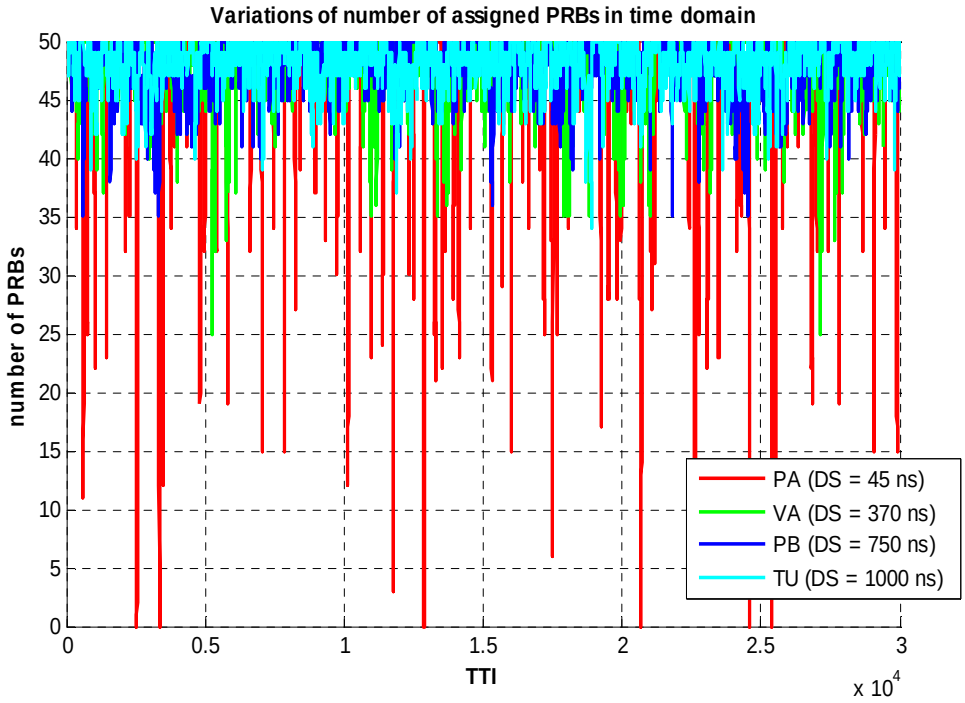

Figure 5.5 Variations of number of assigned PRB in time domain

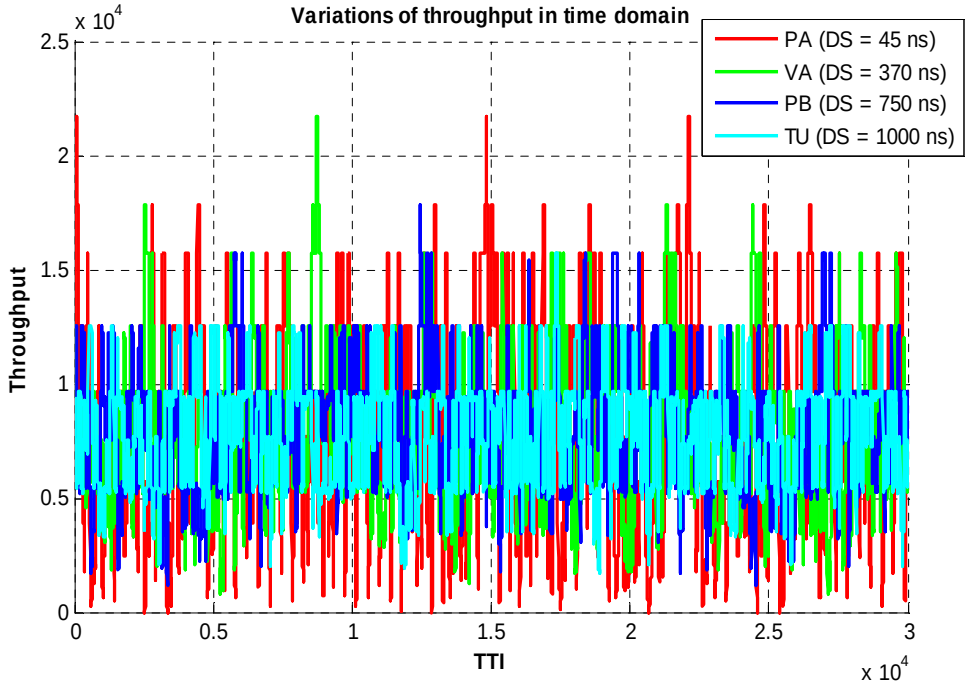

Figure 5.6 Variations of throughput in time domain

5.2.2 Dependencies of LTE system performance on beta

The SISO simulation result as shown in Figure 5.1 was obtained from system level simulation by setting the same set of beta values for all delay spread values. However, in principle beta values should be calibrated from a link level simulation which may result in different beta values for different delay spread values. Due to time limitation and the lack of reliable link level simulator, beta calibration was not done in this study. Nevertheless, some tests were done in order to investigate the sensitivity of LTE system performance with regards to different sets of beta values. Five different sets of beta values were used, i.e. the default beta values as shown in Table 4.3 and four other set of beta values derived by increasing and decreasing the default beta values by certain percentage. According to some literatures, beta value for MCS 1 is in the range between 1 and 2 [33] [34] [35]. Therefore, beta values of 10%, 25% and 50% higher than default beta values together with beta values of 25% lower than the default beta values were considered in this study. These sets of beta values are given in Table 5.2.

The simulation results are shown in Figure 5.7, 5.8, 5.9, and 5.10 for delay spread of 45 ns, 370 ns, 750 ns and 1000 ns respectively. It can be observed that for delay spread of 45 ns, different sets of beta values do not clearly affect LTE system performance while in other higher delay spread values, the LTE system performance is sensitive to the change of beta values especially in the region of high SINR. This is because in delay spread of 45 ns, the frequency channel response is almost flat, and all PRBs have the almost same instantaneous SINR. Thus the effective SINR is more equal to the average of those instantaneous SINR and beta doesn't affect the effective SINR anymore. On the other hand, in the case of higher delay spread, the channel response is more

frequency selective, so the PRB-specific instantaneous SINRs are varying. Thus the effective SINR is more dependent on beta values. This leads to the dependency of throughput on beta values. The SINR gains that can be achieved by different set of beta values in the case of delay spread of 370 ns, 750 ns and 1000 ns are provided in Table 5.3, 5.4 and 5.5 respectively.

Table 5.2 Different sets of beta values

MCS	Default beta	10% higher	25% higher	50% higher	25% lower
0	-999999999.99	-999999999.99	-999999999.99	-999999999.99	-999999999.99
1	1.33	1.46	1.66	2.00	1
2	1.33	1.46	1.66	2.00	1
3	1.33	1.46	1.66	2.00	1
4	1.33	1.46	1.66	2.00	1
5	1.42	1.56	1.78	2.13	1.06
6	1.6	1.76	2.00	2.40	1.2
7	3.8	4.18	4.75	5.70	2.85
8	4.8	5.28	6.00	7.20	3.6
9	6.1	6.71	7.63	9.15	4.57
10	10	11.00	12.50	15.00	7.5
11	15	16.50	18.75	22.50	11.25
12	19.3	21.23	24.13	28.95	14.47
13	25.8	28.38	32.25	38.70	19.35
14	31.3	34.43	39.13	46.95	23.47
15	35	38.50	43.75	52.50	26.25

From Table 5.3, 5.4 and 5.5, it can be observed that the higher the beta values, the higher the SINR gain. But, the SINR gain obtained from those sets of beta values are still low. In other words, even though beta values are obtained from calibration and are in the range as mentioned in Table 5.1, the maximum SINR gain is still less than 1 dB.

Table 5.3 SINR gains obtained from different sets of beta values for Vehicular A

Throughput (Mbps)	SINR gain (dB)			
	Beta 50% higher	Beta 25 % higher	Beta 10% higher	Beta 25% lower
4	0.33	0.20	0.09	-0.32
6	0.40	0.24	0.11	-0.44
8	0.42	0.26	0.12	-0.52
10	0.51	0.32	0.15	-0.54
12	0.52	0.32	0.15	-0.58
14	0.87	0.47	0.13	-0.44

Table 5.4 SINR gains obtained from different sets of beta values for Pedestrian B

Throughput (kbps)	SINR gain (dB)			
	Beta 50% higher	Beta 25 % higher	Beta 10% higher	Beta 25% lower
4	0.38	0.23	0.1	-0.36
6	0.46	0.28	0.13	-0.54
8	0.48	0.29	0.13	-0.59
10	0.56	0.34	0.16	-0.62
12	0.61	0.37	0.17	-0.65
14	0.95	0.51	0.14	-0.52

Table 5.5 SINR gains obtained from different sets of beta values for Typical Urban

Throughput (kbps)	SINR gain (dB)			
	Beta 50% higher	Beta 25 % higher	Beta 10% higher	Beta 25% lower
4	0.39	0.24	0.11	-0.41
6	0.54	0.33	0.15	-0.62
8	0.57	0.36	0.18	-0.74
10	0.63	0.39	0.17	-0.62
12	0.66	0.41	0.19	-0.99
14	0.75	0.31	0.14	-0.62

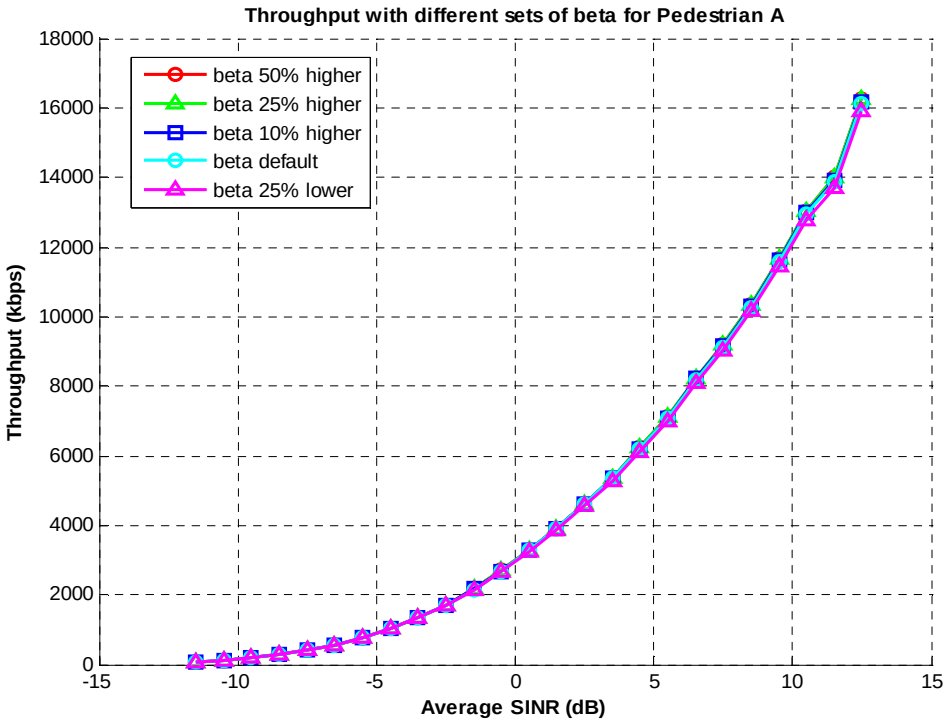

Figure 5.7 Throughput with different sets of beta for Pedestrian A

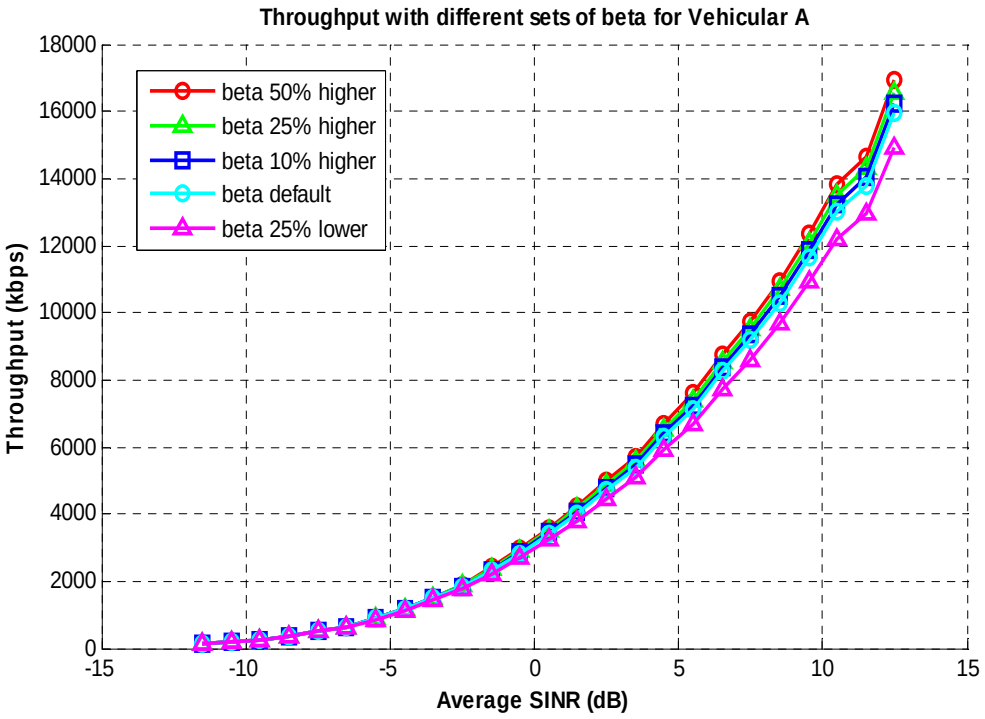

Figure 5.8 Throughput with different sets of beta for Vehicular A

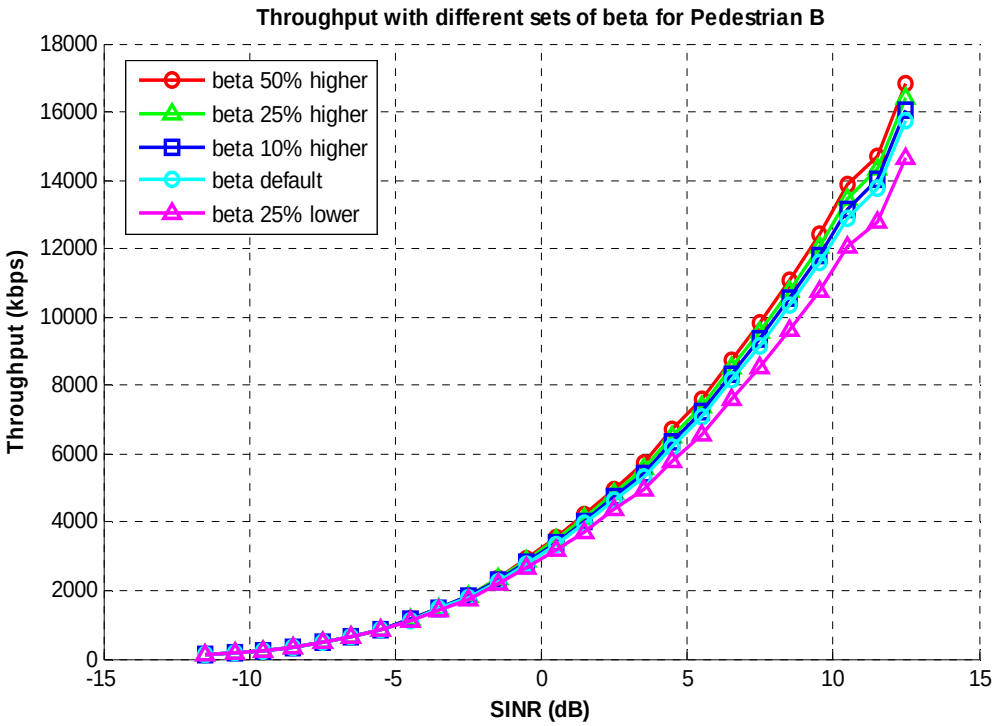

Figure 5.9 Throughput with different sets of beta for Pedestrian B

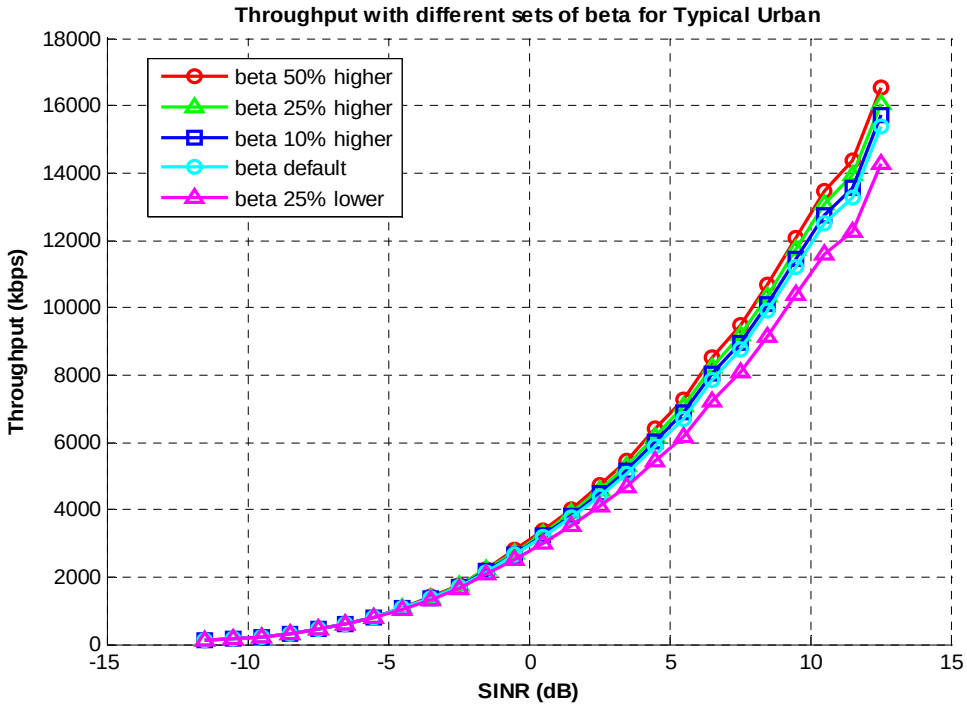

Figure 5.10 Throughput with different sets of beta for Typical Urban

5.2.3 Spatial Correlation Effect on Receive Diversity

In the case of receive diversity the spatial correlation is only at the MS side since BS employs only one antenna. The simulation results for receive diversity taking into account different spatial correlation levels are shown in Figure 5.11. Low correlation corresponds to spatial correlation of 0.19 at the BS and 0.22 at the MS. Medium correlation corresponds to spatial correlation of 0.32 at the BS and 0.79 at the MS. High correlation corresponds to spatial correlation of 1 at the BS and 0.79 at the MS. It can be seen from the figure that for low average SINR the spatial correlation levels do not clearly affect the performance. But, for high average SINR, small difference in throughput can be seen. To achieve a target throughput of 25 Mbps, SINR of 13.79 dB is required in the case of low correlation, 14.16 dB is required in the case of medium correlation and 14.65 dB is required in the case of high correlation. So, SINR gain of 0.86 dB and 0.49 dB are achieved by low and medium correlation respectively. The list of SINR gains for various throughput values are given in Table 5.6.

Table 5.6 SINR gain of receive diversity with low and medium spatial correlation

Throughput (Mbps)	SINR gain (dB)	
	Low correlation	Medium correlation
10	0.17	0.16
15	0.25	0.21
20	0.39	0.29
25	0.86	0.49
30	1.20	0.38

The SINR gains as shown above are achieved because lower correlation means that the channels are less correlated. Thus channels experience different fading, i.e. some channels may experience deep fading but other channels may be in good condition. Consequently, when the same data stream is transmitted over different channels, even though the data stream transmitted through one channel is corrupted due to fading, the data stream transmitted through another channel may be transmitted successfully. This explains why in the case of low correlation and medium correlation the achieved throughput is higher than in the case of high correlation.

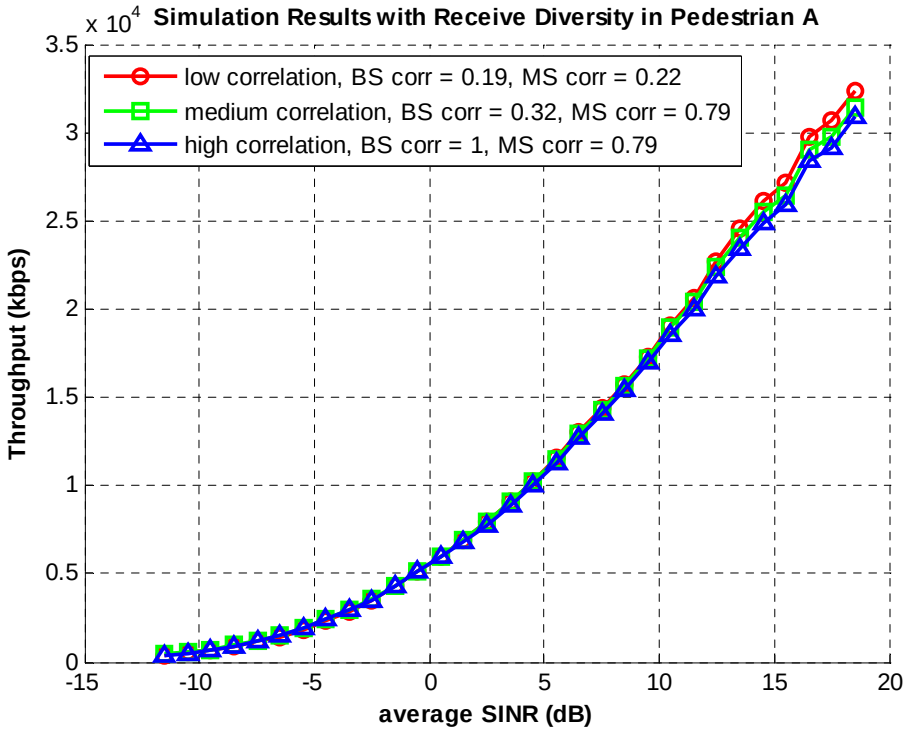

Figure 5.11 System level simulation results with different spatial correlation levels in Receive Diversity scheme

5.2.4 Spatial Correlation Effect on Transmit Receive Diversity

The effect of different spatial correlation levels on the performance of LTE by assuming MIMO transmit receive diversity is shown in Figure 5.12. It can be seen from the figure that lower spatial correlation results in better performance. For instance, to achieve a target throughput of 25 Mbps, in the case of low correlation the required SINR is 13.01 dB, in the case of medium correlation the required SINR is 13.62 dB and in the case of high correlation the required SINR is 14.84 dB. Therefore SINR gain of 1.83 dB and 1.22 dB are achieved by low and medium correlation respectively. The list of SINR gains for some throughput values is given in Table 5.7.

Table 5.7 SINR gain of transmit receive diversity with low and medium spatial correlation

Throughput (Mbps)	SINR gain (dB)	
	Low correlation	Medium correlation
10	0.81	0.45
15	1.04	0.59
20	1.16	0.71
25	1.83	1.22
30	2.19	1.68

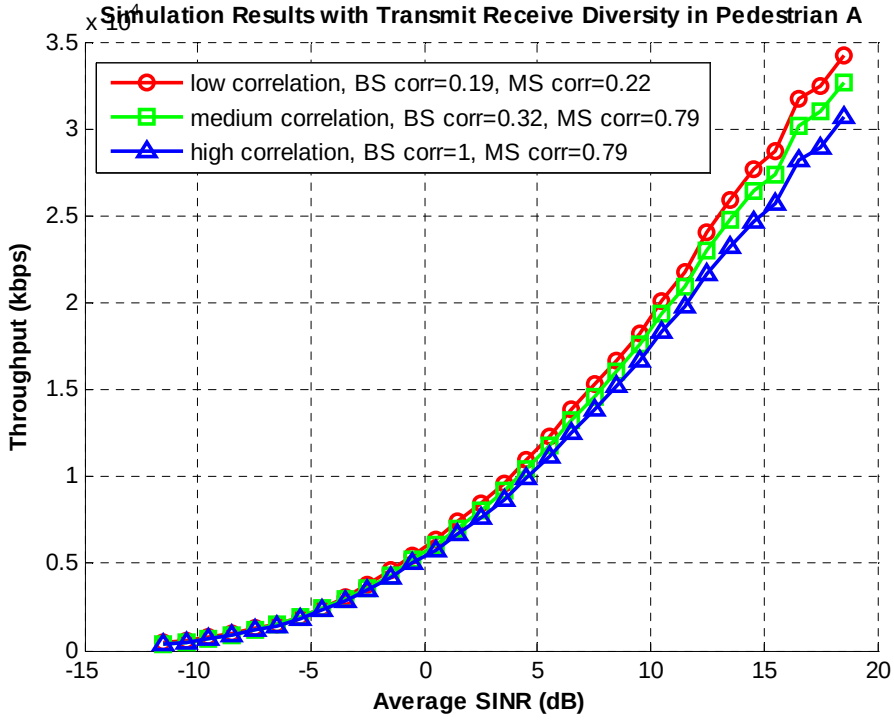

Figure 5.12 System level simulation results with different spatial correlation levels in Transmit Receive Diversity scheme

Comparing the simulation results in both receive diversity and transmit receive diversity shows that the dependency of LTE system performance on spatial correlation levels has similar trends.

The difference is in the SINR gain that can be achieved. This difference in SINR gain is because in receive diversity the performance is affected only by the spatial correlation at the MS side. On the other hand, in the case of transmit receive diversity the performance is affected by the spatial correlation at both the BS and the MS. In the case of high correlation, this might not have any effect because the channels are correlated. But in the case of low and medium correlation, transmit receive diversity exploits diversity gain from the MS side as well as from the BS side. This explains why the SINR gains in the case of transmit receive diversity is higher than those of receive diversity especially in the case of low and medium correlation.

5.2.5 Spatial Correlation Effect on Spatial Multiplexing

Figure 5.13 shows the simulation result with MIMO spatial multiplexing taking into account the effect of spatial correlation. It can be seen clearly that in the case of low correlation, LTE system performance outperforms those in the case of medium and high correlation. Moreover, the SINR gain obtained in the case of spatial multiplexing is higher than the SINR gain obtained from transmit receive diversity. For instance, the required SINRs to achieve throughput of 25 Mbps are 12.62 dB, 14.51 dB and 15.56 dB for low, medium and high correlation respectively. Thus the SINR gain achieved by low spatial correlation is 2.94 dB and the SINR gain achieved by medium spatial correlation is 1.05 dB. The list of SINR gain for various throughput values in the case of spatial multiplexing is given in Table 5.8.

Table 5.8 SINR gain of spatial multiplexing with low and medium spatial correlation

Throughput (Mbps)	SINR gain (dB)	
	Low correlation	Medium correlation
10	3.17	2.02
15	3.44	2.12
20	3.88	2.3
25	2.94	1.05
30	2.44	1.51

Although SINR gain achieved from different spatial correlation levels in the case of spatial multiplexing is higher than those achieved in transmit receive diversity, the required SINR to achieve throughput of 25 Mbps is higher for SM especially in the case of high and medium correlation. This is because spatial multiplexing needs high SINR in order to result in the best performance as shown in Figure 5.14. The smooth curves correspond to simulation results with spatial multiplexing and the dashed curves correspond to simulation results with transmit receive diversity. In the case of low correlation, spatial multiplexing outperforms transmit receive diversity for SINR higher than 11.5 dB, in the case of medium correlation spatial multiplexing outperforms transmit receive diversity for SINR higher than 14.8 dB and in the case of high correlation, spatial multiplexing outperforms transmit receive diversity only for SINR higher than 16.6 dB. These crossing SINRs are close to the one investigated in [36] which is 15 dB.

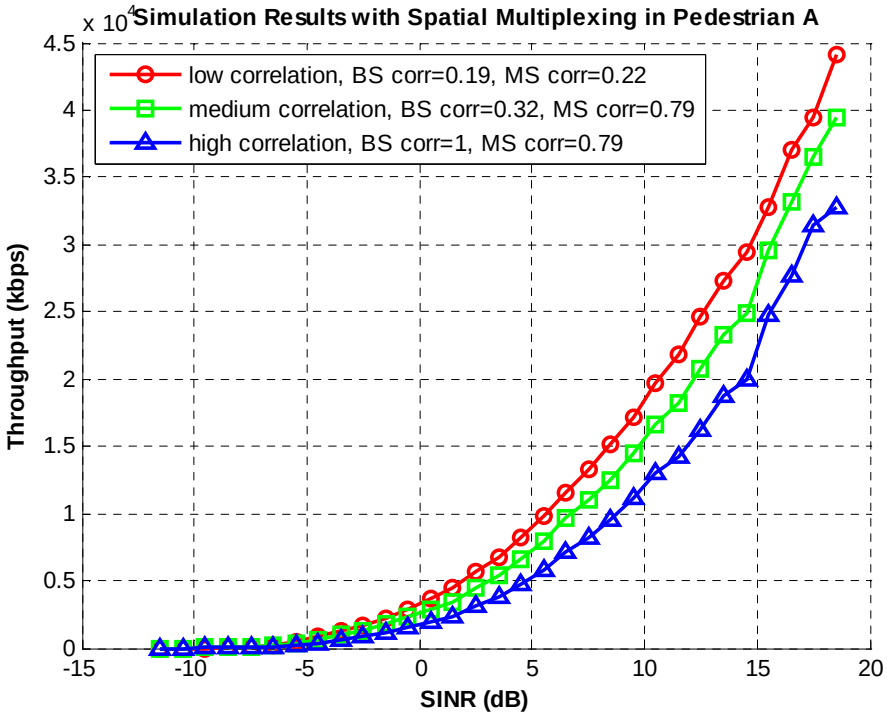

Figure 5.13 System Level Simulation results with different spatial correlation levels in spatial multiplexing mode

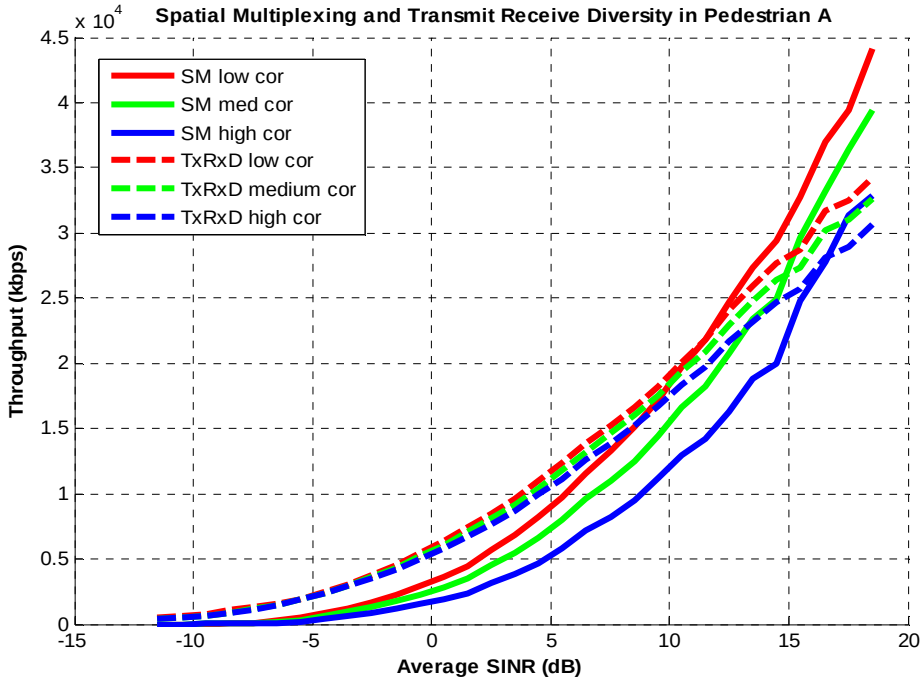

Figure 5.14 Comparison between system level simulation results with spatial multiplexing and transmit receive diversity

5.2.6 Angular Spread Effect on Spatial Multiplexing

Angular spread is a factor which determines spatial correlation between antenna elements. In this study, the effect of per path angular spread at the MS on LTE system performance is investigated in MIMO Spatial Multiplexing. Three different values are investigated, i.e. 35, 5 and 2 degree. MS side per path angular spread of 35 degree corresponds to spatial correlation of 0.79 whereas per path angular spread of 5 and 2 degree corresponds to spatial correlation of 1. The spatial correlation at the BS side in all cases is 0.32. The simulation result is depicted in Figure 5.15. It shows that per path angular spread at mobile station strongly affect the performance of LTE. This is due to high spatial correlation introduced by small per path angular spread value. While large per path angular spread value results in low correlation, hence the performance of spatial multiplexing is better than those of low per path angular spread values.

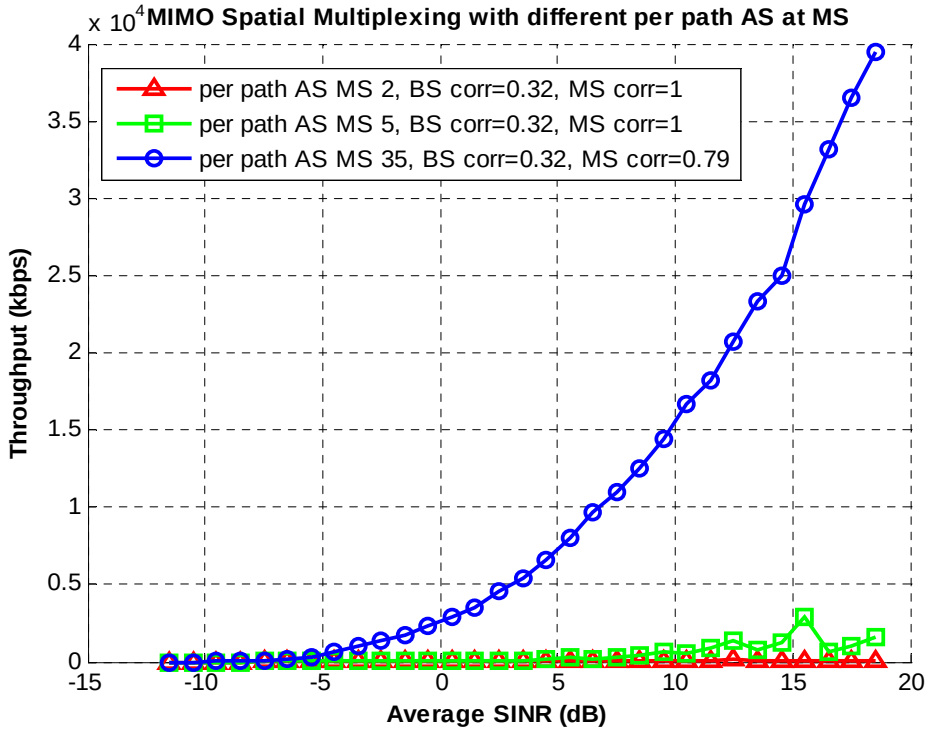

Figure 5.15 System level simulation results with different spatial correlation levels in spatial multiplexing scheme

5.3 Recommendations for radio planning

The simulation results and the analysis of LTE system performance in relation to wideband channel properties have been provided in the previous section. Based on the simulation results for different delay spread values and different angular spread values, this section provides recommendations for LTE radio planning as follows:

1. The simulation results indicate that delay spread is not so important to be included in the radio planning. By considering the implementation of AMC and assuming the same set of beta values for all delay spread values, the simulation results show that LTE performance in terms of throughput is not clearly affected by delay spread values. Moreover, some tests were done in order to investigate the dependencies of LTE performance on beta values. The results show that the achieved SINR gains for various throughput values are less than 1 dB.
2. First simulation results on the effect of per path angular spread on LTE performance shows that LTE performance is strongly affected by per path angular spread value. This indicates that the SINR gain introduced by different per path angular spread values is important to be included in radio planning. But due to the limited data obtained from this study, the list of SINR gain for certain target throughput cannot yet be provided. Further simulations are required to derive quantitative results for SINR gain that can be used in radio planning.

Chapter 6
Conclusions and Recommendations

6.1 Conclusions

In this study, the investigation on the effect of wideband channel properties on LTE system performance were done by performing LTE system level simulation. LTE system level simulation models AMC (Adaptive Modulation and Coding). Thus it aligns with how the system works in reality. In order to implement AMC, the system level simulation needs an accurate estimate of link level performance in terms of BLER. For this reason, AWGN link level simulation is required.

LTE uses OFDM as one of the key technologies. The system bandwidth is divided into many subcarriers. Furthermore subcarriers are grouped into PRB which is the smallest resource allocated to a user. Due to frequency selective fading, PRBs assigned to the user may have different instantaneous SINRs. Meanwhile, one SINR value is required to determine the modulation and coding scheme. In this study, EESM (Exponential Effective SINR Mapping) is chosen as a method to map per-PRB instantaneous SINR into single SINR value called effective SINR. An important parameter used to determine SINR effective in EESM is beta which in principle needs to be calibrated from link level simulation.

From the system level simulation results and the analysis of LTE system performance in relation to wideband channel properties, conclusions are derived as follows:

1. *Delay spread doesn't significantly affect LTE system performance in terms of average throughput.* Average througput is throughput obtained by averaging out over 30000 TTI. In this study, the first investigation was done by using the same set of beta values for different delay spread values, i.e. 45, 370, 750 and 1000 ns. The result shows that the performance of LTE is not clearly affected by delay spread values. Then, some tests were performed in order to investigate the dependencies of LTE performance on beta values. The results show that the SINR gains achieved by varying beta values are less than 1 dB. Thus, it indicates that delay spread is not so important to be included in LTE radio planning.
2. *Per path angular spread strongly affects LTE system performance*. First investigation on the effect of per path angular spread on LTE system performance was done by considering MIMO Spatial Multiplexing. The result show that LTE performance in terms

of throughput is significantly affected by per path angular spread values. Higher per path angular spread value leads to better LTE performance due to lower spatial correlation. On the other hand, lower per path angular spread value leads to worse performance. In the case of low angular spread (2 and 5 degree) the achieve throughput is almost 0. This indicates that it is important to include per path angular spread in LTE radio planning.

3. *Spatial correlation between channel elements affects LTE system performance.* Investigations on the effect of spatial correlation on LTE system performance were done by considering receive diversity (SIMO), MIMO transmit receive diversity and MIMO spatial multiplexing. In general, the effect of spatial correlation on LTE performance for those modes is same, i.e. lower correlation results in better performance. The difference is in the amount of SINR gain that can be obtained. The highest gain is obtained by implementing MIMO spatial multiplexing which can achieve SINR gain up to 3.88 dB, then followed by transmit receive diversity which can achieve SINR gain up to 2.19 dB. The smallest SINR gain is obtained from receive diversity (SIMO) which can achieve SINR gain up to 1.2 dB.
4. *Spatial Multiplexing outperforms Transmit Receive Diversity in the case of high SINR.* Even though the SINR gain obtained by implementing MIMO spatial multiplexing is higher than that obtained by implementing MIMO transmit receive diversity, the required SINRs in the case of spatial multiplexing to achieve some throughput values are higher than the required SINRs in the case of transmit receive diversity. This is because spatial multiplexing requires high SINR in order to result in the best performance. In the case of low correlation, spatial multiplexing outperforms transmit receive diversity for SINR higher than 11.5 dB, in the case of medium correlation, spatial multiplexing outperforms transmit receive diversity for SINR higher than 14.8 dB, and in the case of high correlation, spatial multiplexing outperforms transmit receive diversity for SINR higher than 16.6 dB.

6.2 Recommendations for further study

Some recommendations are provided for further study in this topic as follows:

1. A validation of the simulation results is proposed by doing real measurements. The real measurement of LTE performance can be done during the LTE trial that will be conducted by TNO in September 2011.
2. In this study, the duration of a simulation is 30000 TTI which equals to 30 s. In reality the duration of a file download is 1 s (1000 TTI) in average. Hence, for the next study, the simulations for duration of 1 s are recommended. With the duration of 1 s, the average throughput for different delay spread values might not be the same.
3. Three per path angular spread values, i.e. 2, 5 and 35 degree are taken into account in the investigation on the effect of per path angular spread value on LTE performance. Moreover only MIMO spatial multiplexing is considered. Therefore, for further study, more investigations on per path angular spread effect by considering SIMO and MIMO

transmit diversity and taking into account more per path angular spread values should be done.

4. The investigation on the effect of delay spread in this study was done by using the beta values provided in [33]. Thus for the further study, a beta calibration per multipath propagation model is proposed to be done in order to get more accurate beta values for every delay spread values. This would require a link level simulator.

Appendix A

Instantaneous SINR Calculation

1. Transmit Receive Diversity

In general, the system can be represented as shown in figure A.1. The per-PRB instantaneous SINR in the case of transmit receive diversity is given by:

$$SINR_{b,m} = \frac{\left(\hat{P}^{rx}_{b,m,A,1} + \hat{P}^{rx}_{b,m,A,2} + \hat{P}^{rx}_{b,m,B,1} + \hat{P}^{rx}_{b,m,B,2}\right)^2}{\left[\begin{array}{l}\left(\hat{P}^{rx}_{b,m,A,1} + \hat{P}^{rx}_{b,m,B,1}\right)\sum_{\text{sector}\ b'\neq b}\left(\tilde{P}^{rx}_{b',m,A,1} + \tilde{P}^{rx}_{b',m,B,1}\right)+ \\ \left(\hat{P}^{rx}_{b,m,A,2} + \hat{P}^{rx}_{b,m,B,2}\right)\sum_{\text{sector}\ b'\neq b}\left(\tilde{P}^{rx}_{b',m,A,2} + \tilde{P}^{rx}_{b',m,B,2}\right)+ \\ \left(\hat{P}^{rx}_{b,m,A,1} + \hat{P}^{rx}_{b,m,A,2} + \hat{P}^{rx}_{b,m,B,1} + \hat{P}^{rx}_{b,m,B,2}\right)N\end{array}\right]} \quad (1)$$

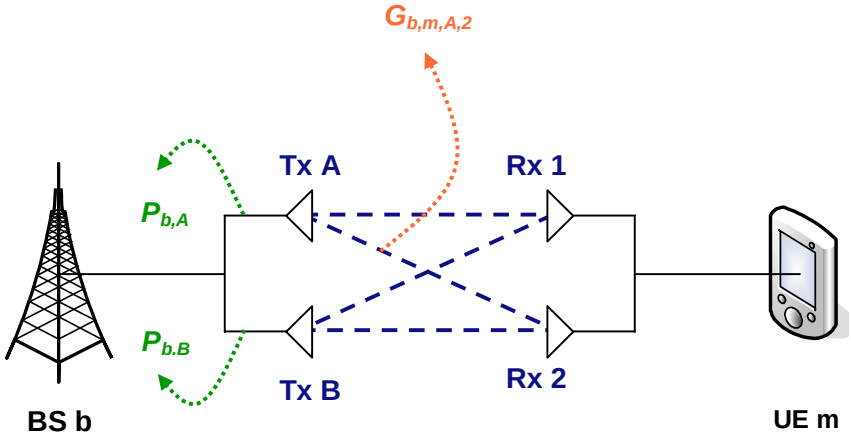

Figure A.1. Overview of the system in general

Where $\hat{P}^{rx}_{b,m,A,1} \equiv \hat{P}_{b,A} G_{b,m,A,1}$ is the received signal power level from BS b transmit antenna A at the UE m received antenna 1, $\tilde{P}^{rx}_{b',m,A,1} \equiv \tilde{P}_{b',A} G_{b',m,A,1}$ the received interference power level from BS b' transmit antenna A at UE m receive antenna 1.

2. Spatial Multiplexing

In the case of spatial multiplexing, two codewords are transmitted from two different transmit antennas at the same time. The per-PRB SINR is calculated as follows:

$$SINR = \frac{1}{(|b_{n1}|^2 + |b_{n2}|^2)\sigma^2 + \sum_{m=1}^{N_{\mathrm{INT}}} (|c_{n1}|^2 + |c_{n2}|^2)_m}, \forall n \quad (2)$$

where

$$C_m^{odd} = \begin{bmatrix} \frac{1}{2}(h_{11} - h_{12}) & \frac{1}{2}(h_{11} + h_{12}) \\ \frac{1}{2}(h_{21} - h_{22}) & \frac{1}{2}(h_{21} + h_{22}) \end{bmatrix}_0^+ \begin{bmatrix} \frac{1}{2}(h_{11} - h_{12}) & \frac{1}{2}(h_{11} + h_{12}) \\ \frac{1}{2}(h_{21} - h_{22}) & \frac{1}{2}(h_{21} + h_{22}) \end{bmatrix}_m$$

$$C_m^{even} = \begin{bmatrix} \frac{1}{2}(h_{11} + h_{12}) & \frac{1}{2}(h_{11} - h_{12}) \\ \frac{1}{2}(h_{21} + h_{22}) & \frac{1}{2}(h_{21} - h_{22}) \end{bmatrix}_0^+ \begin{bmatrix} \frac{1}{2}(h_{11} + h_{12}) & \frac{1}{2}(h_{11} - h_{12}) \\ \frac{1}{2}(h_{21} + h_{22}) & \frac{1}{2}(h_{21} - h_{22}) \end{bmatrix}_m$$

$$B^{odd} = \begin{bmatrix} \frac{1}{2}(h_{11} - h_{12}) & \frac{1}{2}(h_{11} + h_{12}) \\ \frac{1}{2}(h_{21} - h_{22}) & \frac{1}{2}(h_{21} + h_{22}) \end{bmatrix}_0^+$$

$$B^{even} = \begin{bmatrix} \frac{1}{2}(h_{11} + h_{12}) & \frac{1}{2}(h_{11} - h_{12}) \\ \frac{1}{2}(h_{21} + h_{22}) & \frac{1}{2}(h_{21} - h_{22}) \end{bmatrix}_0^+$$

3. Receive Diversity

In the case of receiver diversity, the number of transmit antenna is one and the number of receive antenna is two. The receiver combines the signals at two receive antennas by Maximal Ratio Combining (MRC). Thus the per-PRB instantaneous SINR is calculated according to:

$$\begin{aligned} SINR_{b,m} &= SINR_{b,m,A,1} + SINR_{b,m,A,2} \\ &= \frac{\hat{P}_{b,A} G_{b,m,A,1}}{\sum_{\text{sector } b' \neq b} \left(\tilde{P}_{b',A} G_{b',m,A,1} + \tilde{P}_{b',B} G_{b',m,B,1} \right) + N} + \frac{\hat{P}_{b,A} G_{b,m,A,2}}{\sum_{\text{sector } b' \neq b} \left(\tilde{P}_{b',A} G_{b',m,A,2} + \tilde{P}_{b',B} G_{b',m,B,2} \right) + N} \end{aligned} \quad (3)$$

Appendix B
LTE Link Level Simulation

During the study, LTE link level simulation in AWGN level was also performed. The simulation was done by using a Matlab-based simulator developed by Antcor[1]. The simulation was done for system bandwidth of 1.4 MHz, hence there are 6 PRBs. It is assumed that there is only one user and the transmission mode is SISO. The simulation lasts for duration of 5000 subframe and normal cyclic prefix is inserted in each OFDM symbol. During data transmission, it is also assumed that there is no HARQ retransmission. Eight different combinations of modulation and transport block size as shown in Table B.1 are simulated. The modulation order 2 corresponds to QPSK modulation and higher transport block size index means longer transport block size.

Table B.1 Mapping MCS index to modulation order and TBS index [15]

MCS Index	Modulation order	TBS index
0	2	0
1	2	1
2	2	2
3	2	3
4	2	4
5	2	5
6	2	6
7	2	7
8	2	8

The simulation results in terms of BLER (Block Error Rate) and throughput are shown in Figure B.1. It can be seen from the result that higher MCS requires higher SNR in order to achieve the same block error rate. In other words, with the same SNR, higher MCS result in higher block error rate. Since the modulation is the same for all MCS index, this is due to higher MCS corresponds to longer transport block size. Therefore it needs higher power to achieve a certain block error rate.

Due to the incompatibility with system level simulator used in this study, this link level simulation result is not used in the approach of this study. The incompatibility is that this link level simulator determines the modulation and coding scheme based on MCS index which

[1] Name of the company which developed the simulator, further information can be found here: http://www.antcor.com/

represent the modulation order and transport block size index. On the other hand, the system level simulator determines the modulation and coding scheme based on CQI (Channel Quality Indicator). Therefore, AWGN link level simulation result used in this study is referring to [32].

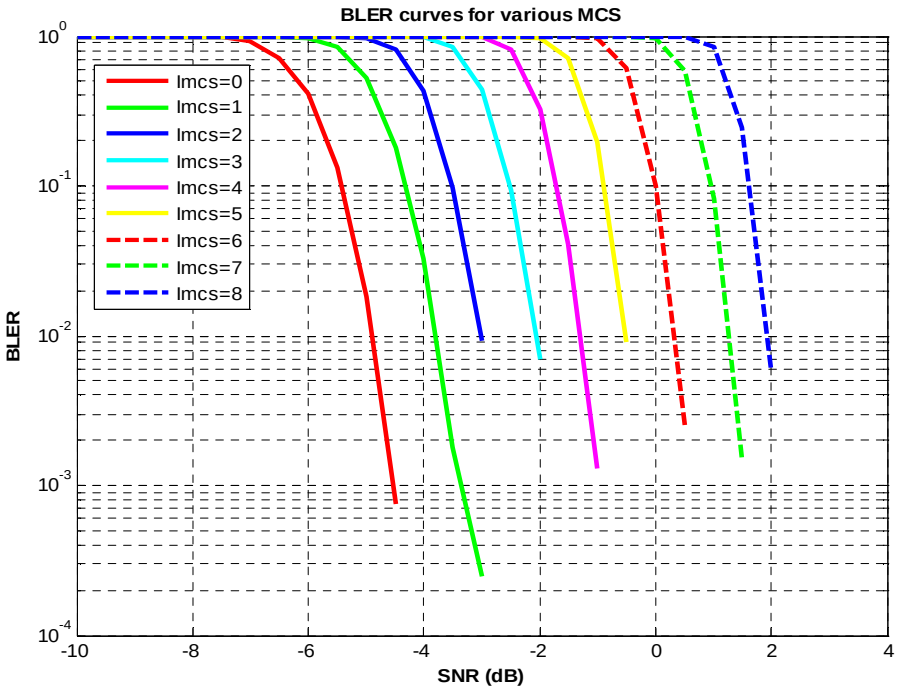

Figure B.1 LTE link level simulation in terms of BLER

Bibliography

[1] Global Mobile Suplier Association, GSM/3G Market/Technology Update, May 11, 2001.

[2] E. Biglieri, R. Calderbank, A. Constantinides, A. Goldsmith, A. Paulraj, and H.V. Poor, "*MIMO Wireless Communications*", Cambridge University Press, 2007.

[3] D. Gesbert, et.al, "From Theory to Practice: An overview of MIMO space-time coded wireless systems", *IEEE Journal On Selected Areas In Communications*, Vol. 21, No. 3, April 2003

[4] 3GPP Document TR 25.996, "Spatial Channel Model for MIMO simulation (release 7)".

[5] 3GPP Document TS 36.104, "E-UTRAN: Base Station (BS) radio transmission and reception.

[6] J.C.-I. Chuang, "The effect of time delay spread on portable radio communications channel with digital modulation", *IEEE journal on selected areas in communications*, SAC-5(5), June 1987.

[7] A. van Zelst and J. Hammerschmidt, "*A single coefficient spatial correlation model for multiple input multiple output (MIMO) radio channels*, [online]. Available: http://citeseerx.ist.psu.edu/viewdoc/summary?doi=10.1.1.139.3416&rank=3

[8] Pu Li, "OFDM Performance in Relation to Wideband Channel Properties", M.Sc. thesis TU Eindhoven, August 2009.

[9] D.M. Balston and R.C.V. Macario, "*Cellular Radio System*,Artech House Inc., 2003

[10] S. Sesia, I. Toufik, M. Baker, *LTE-The UMTS Long Term Evolution From Theory to Practices*, John Wiley and Sons, Ltd, 2009.

[11] 3GPP Document TR 25.913, "Requirement for Evolved UTRA (E-UTRA) and Evolved UTRAN (E-UTRAN) (release 9)".

[12] 3GPP Document TS 36.211, "Evolved Universal Terrestrian Radio Access (EUTRA); Physical Channel and Modulation (release 8)".

[13] G.J. Foschini and M.J. Gans, "On limits of wireless communications in a fading environment when using multiple antennas," *Wireless Personal Communications*, vol. 6, pp. 311-335, March 1998

[14] E. Telatar, "Capacity of Multi-Antenna Gaussian Channels," technical memorandum, AT&T Bell Laboratories, June 1995.

[15] H. Nikookar, "*Advanced Topics in Digital Wireless Communication*", IRCTR-Delft University of Technology, March 2004.

[16] 3GPP Document TS 36.213 "Evolved Universal Terrestrial Radio Access (EUTRA); Physical Layer Procedure (release 8)."

[17] LTEWorld, *The Seven Modes of MIMO in LTE*, [online]. Available: http://lteworld.org/whitepaper/seven-modes-mimo-lte

[18] J. Zyren, "Overview of the 3GPP Long Term Evolution Physical Layer", Freescale Semiconductor, Inc.

[19] B. Sklar, "Rayleigh Fading Channels in Mobile Digital Communication Systems Part I: Characterization", *IEEE Communication Magazine*, July 1997.

[20] Recommendation ITU-R M.125, "Guidelines for Evaluation of Radio Transmission Technologies for IMT-2000".

[21] M.R.J.A.E. Kwakkernaat, "Angular Dispersion of Radio Waves in Mobile Channels: Measurement-based Analysis and Modelling", Ph.D. thesis TU Eindhoven, December 2008.

[22] T. Rautiainen, G. Wölfle, and R. Hoppe, "Verivying path loss and delay spread predictions of a 3D ray tracing propagation model in urban environment", Proc. *IEEE Vehicular Technology Conference 2002-Fall.* Page(s): 2470-2474, vol.4.

[23] P. Svedman, S.K. Wilson, L.J. Cimini, and B.Ottersten, "A simplified opportunistic feedback and scheduling scheme for OFDM", *VTC 2004 Spring*, pp.1878-1882, 2004.

[24] K. Zhou and Y.H. Chew, "On the achievable diversity gain by the optimal subcarrier allocations in multiuser OFDM system," *Proc. Of IEEE MILCOM 2006*, pp. 1-6, Oct 2006.

[25] T.C.W. Schenk, G. Dolmans, and I. Modonesi, "Throughput of a MIMO OFDM based WLAN", *Proc. of SCVT'2004*, November 2004.

[26] D. Shan Shiu, G.J. Foschini, M.J. Gans, J.M. Khan and S. Member, "Fading correlation and its effect on the capacity of multielement antenna systems, "*IEEE Trans. Commun*, vol. 48, pp. 502-513, 2000.

[27] 3GPP Document TR 25.996, "Spatial channel model for multiple input multiple output (MIMO) simulations (release 8)", 2009.

[28] S. Pan, S. Durrani, and M.E. Bialkowski, "MIMO Capacity of Spatial Channel Model Scenarios", *IEEE Australian Communications Theory Workshop*, 2007.

[29] A. Goldsmith, *Wireless Communication*, Cambridge University Press, 2005.

[30] E. Dahlman et al., "Key features of LTE radio interface", Ericsson review no.2, 2008.

[31] 3GPP Document TS 36.101, "Evolved Universal Terrestrial Radio Access (EUTRA); User Equipment (UE) radio transmission and reception (release 8)."

[32] J.C. Ikuno, M. Wrulich and M. Rupp, "System Level Simulation of LTE networks", *IEEE 71st Vehicular Technology Conference: VTC 2010-Spring*, 16-19 May 2010.

[33] A. Oborina, M. Moisio, V. Koivunen, "Ergodic System Capacity of Mobile MIMO System using Adaptvie Modulation", *21st Annual IEEE International Symposium on Personal, Indoor and Mobile Radio Communications*, 2010.

[34] J. Olmos, et al., "Exponential Effective SIR Metric for LTE Downlink", *IEEE 20th International Symposium on Personal, Indoor and Mobile Radio Communications*, 2009.

[35] 3GPP Document TR 25.892, "Feasibility study for OFDM for UTRAN enhancement (release 6)," March 2004.

[36] C. F. Ball, E.Humburg, S. Eder and L. Lacinak, "Wimax Capacity Enhancements introducing MIMO 2x2 Diversity and Multiplexing", *IEEE Mobile and Wireless Communication Summit*, 2007.